Mapping the suitability of groundwater dependent vegetation in a semi-arid Mediterranean area

Inês Gomes Marques[1]; João Nascimento[2]; Rita M. Cardoso[1]; Filipe Miguéns[2]; Maria Teresa Condesso de Melo[2]; Pedro M. M. Soares[1]; Célia M. Gouveia[1]; Cathy Kurz Besson[1]

[1] Instituto Dom Luiz; Faculty of Sciences, University of Lisbon, Campo Grande, Ed. C8, 1749-016, Lisbon, Portugal

[2] CERIS; Instituto Superior Técnico, University of Lisbon, 1049-001, Lisbon, Portugal

Correspondence to: Inês Gomes Marques (icgmarques@fc.ul.pt)

Abstract.

In this study, we modeled the distribution of deep-rooted woody species in southern Portugal from climatic, hydrological and topographic environmental variables. To achieve this, we first relied on the density of *Quercus suber, Quercus ilex* and *Pinus pinea* as proxy species of GDV. Model fitting was performed between the proxy species Kernel density and the selected environmental predictors using 1) a simple linear model and 2) a Geographically Weighted Regression (GWR), to account for auto-correlation of the spatial data and residuals. When comparing the results of both models, the GWR modelling results showed improved goodness of fitting, as opposed to the simple linear model. Climatic indices were the main drivers of GDV density closely followed by groundwater depth, drainage density and slope. Groundwater depth did not appear to be as pertinent in the model as initially expected, accounting only for about 6% of the total variation against 89% for climate drivers.

The relative proportions of model predictor coefficients were used as weighting factors for multicriteria analysis, to create a suitability map to the GDV in southern Portugal showing where the vegetation is most likely to rely on groundwater to cope with aridity. A validation of the resulting map was performed using independent data of the Normalized Difference Water Index (NDWI) a satellite-derived vegetation index. NDWI anomalies were calculated for June, July and August of 2005 in reference to years 1999-2009 to assess the response of active woody species in the region after an extreme drought. The results from the NDWI anomaly provided an overall good agreement between areas with good or bad suitability to host GDV. The model was considered reliable to predict the distribution of the studied vegetation. However, lack of data quality and information were shown to be the main cause for suitability discrepancies between maps.

The methodology developed to map GDV's will allow to predict the evolution of the distribution of GDV according to climate change scenarios and aid stakeholder decision-making concerning priority areas of water resources management.

Keywords: Groundwater dependent ecosystems, aridity, agroforestry, suitability map.

1 Introduction

Mediterranean forests, woodlands and shrublands, mostly growing under restricted water availability, are one of the terrestrial biomes with higher volume of groundwater used by vegetation (Evaristo and McDonnell, 2017). Future predictions of decreased precipitation (Giorgi and Lionello, 2008; Nadezhdina et al., 2015), decreased runoff (Mourato et al., 2015) and aquifer recharge (Ertürk et al., 2014; Stigter et al., 2014) in the Mediterranean region threaten the sustainability of groundwater reservoirs and the corresponding dependent ecosystems. Therefore, a sustainable management of groundwater resources and the Groundwater Dependent Ecosystems (GDE) is of crucial importance.

Mapping GDE constitutes a first and fundamental step to their active management. Several approaches have been proposed, including remote sensing techniques (e.g. Normalized Difference Vegetation Index – NDVI) (Barron et al., 2014; Eamus et al., 2015; Howard and Merrifield, 2010), remote-sensing combined with ground-based observations (Lv et al., 2013), based on geographic information system (GIS) (Pérez Hoyos et al., 2016a) or statistical approaches (Pérez Hoyos et al., 2016b). An integrated multidisciplinary methodology (Condesso de Melo et al., 2015) has also been used. A widely used classification of GDE was proposed by Eamus et al. (2006). This classification distinguishes three types: 1) Aquifer and cave ecosystems, which includes all subterranean waters; 2) Ecosystems reliant on surface groundwater (e.g. estuarine systems, wetlands; riverine systems) and 3) Ecosystems reliant on subsurface groundwater (e.g. systems where plants remain physiologically active during extended drought periods, without visible water source).

Despite of a wide-ranging body of literature regarding GDE, most of the studies do not include Mediterranean regions (Doody et al., 2017; Dresel et al., 2010; Münch and Conrad, 2007). Moreover, studies on ecosystems relying on subsurface groundwater frequently only focused on riparian environments (Lowry and Loheide, 2010; O'Grady et al., 2006), with few examples in Mediterranean areas (del Castillo et al., 2016; Fernandes, 2013; Hernández-Santana et al., 2008; Mendes et al., 2016). There is a clear knowledge gap concerning the identification of such ecosystems, their phreatophyte associated vegetation (Robinson, 1958) in the Mediterranean region and the management actions that should be taken to decrease the adverse effects of climate change.

In the driest regions of the Mediterranean basin, the persistent lack of water during the entire summer periods selected plants with drought-avoiding strategies, like those that reach deeper stored water up to the point of relying on groundwater (Canadell et al., 1996; Miller et al., 2010). Groundwater access by deep rooting species is often associated to hydraulic lift and/or hydraulic redistribution mechanisms (Orellana et al., 2012). Those mechanisms provide the ability to move water from deep soil layers, where water content is higher, to more shallow layers where water content is lower (Horton and Hart, 1998; Neumann and Cardon, 2012). Hydraulic lift and redistribution have been reported for several woody species of the Mediterranean basin (David et al., 2007; Filella and Peñuelas, 2004) and noticeably for Cork oak (*Quercus suber* L.) (David et al., 2013; Kurz-Besson et al., 2006; Mendes et al., 2016).

Cork oak woodlands are agro-silvo-pastoral systems of the southwest Mediterranean basin (Joffre et al., 1999) that have already been referenced has a groundwater dependent terrestrial ecosystem (Mendes et al., 2016). In the ecosystems of this geographical area, the dominant tree species are the cork oak (*Quercus suber* L.) and the Portuguese holm oak (*Quercus ilex* subs *rotundifolia* Lam.) (Pinto-Correia et al., 2011). Additionally, stone pine (*Pinus pinea* L.) has become a commonly co-occurrent species in the last decades (Coelho and Campos, 2009). The use of groundwater has been frequently reported for both Pinus (Filella and Peñuelas, 2004; Grossiord et al., 2016; Peñuelas and Filella, 2003) and Quercus (Barbeta and Peñuelas, 2017; David et al., 2007, 2013, Kurz-Besson et al., 2006, 2014; Otieno et al., 2006) genre. Furthermore, the contribution of groundwater to tree physiology has been shown to be of a greater magnitude for *Quercus* sp. as compared with *Pinus* sp. (del Castillo et al., 2016; Evaristo and McDonnell, 2017).

Q. suber and *Q. ilex* have been associated with high resilience and adaptability to hydric and thermic stress, and to recurrent droughts in the southern Mediterranean basin (Barbero et al., 1992). In Italy and Portugal, during summer droughts *Q. ilex* used a mixture of rain-water and groundwater and was able to take water from very dry soils (David et al., 2007; Valentini et al., 1992). An increasing contribution of groundwater in the summer has also been shown for this species (Barbeta et al., 2015). Similarly, *Q. suber* showed a seasonal shift in water sources, from shallow soil water in the spring to the beginning of the dry period followed by a progressive higher use of deeper water sources throughout the drought period (Otieno et al., 2006). In addition, the species roots are known to reach depths as deep as 13m in southern Portugal (David et al., 2004). Although co-occurrent to cork and holm oaks species, there is still no evidence yet that *P. pinea* relies on groundwater resources during the dry season. However it shows a very similar root system (Montero et al., 2004) as compared to cork oak (David et al., 2013), with large sinker roots reaching 5 m depth (Canadell et al., 1996). Given the information available on water use strategies by the phreatophyte arboreous species of the cork oak woodlands, we considered *Q. ilex*, *Q. suber* and *P. pinea* as proxies for vegetation that belongs to GDE relying on subsurface groundwater (from here onwards designed as Groundwater Dependent Vegetation – GDV).

GDV of the Mediterranean basin is often neglected in research. Indeed, still little is known about the GDV distribution, but research has already been done on the effects of climate change in specific species distribution, such as *Q. suber*, in the Mediterranean basin (Duque-Lazo et al., 2018; Paulo et al., 2015). While the increase in atmospheric CO_2 and the raising temperature can boost tree growth (Barbeta and Peñuelas, 2017; Bussotti et al., 2013; Sardans and Peñuelas, 2004), water stress can have a counteracting effect on growth of both *Quercus ilex* (López et al., 1997; Sabaté et al., 2002) and *P. pinaster* (Kurz-Besson et al., 2016). Therefore, it is of crucial importance to identify geographical areas where subsurface GDV is present and characterize the environmental conditions this vegetation type is thriving in. This would contribute to the understanding of how to manage these species under unfavorable future climatic conditions.

The aim of this study was to create a suitability map of the current distribution of the arboreous phreatophyte species considered here as GDV in southern Portugal, based on the occurrence of known and foreseen subsurface phreatophyte species and well-known environmental conditions affecting water resources availability. Several environmental predictors were selected according to their impact on water use and storage and then used in a Geographically Weighted Regression (GWR) to model the density of *Q. suber*, *Q. ilex* and *P. pinea* occurrence in the Alentejo region (NUTSII) of southern Portugal. So far, very few applications of this method have been used to model species distribution and only recently its use has spread in ecological research (Hu et al., 2017; Li et al., 2016; Mazziotta et al., 2016). The coefficients proportions obtained from the model equation for each predictor were used as weights to build the suitability map with GIS multi-factor analysis, after reclassifying each environmental predictor.

Based on the environmental conditions of the study area and the species needs, we hypothesized that 1) groundwater depth together with climatic conditions play one of the most important environmental roles in GDV's distribution and 2) groundwater depth between 1.5 and 15m associated with xeric conditions should favor a higher density of GDV and thus a larger use of groundwater by the vegetation.

2 Material and Methods

2.1 Study area

The administrative region of Alentejo (NUTSII) (fig01) covers an area of 31 604.9 km^2, between the latitude 37.22º to 39.39º N and longitude 9.00º to 6.55º W. This study area is characterized by a Mediterranean temperate mesothermic climate with hot and dry summers, defined as Csa in the Köppen classification (APA, n.d.; ARH Alentejo, 2012a, 2012b). It is characterized by a sub-humid climate, which has recently quickly drifted to semi-arid conditions (Ministério da Agricultura do Mar do Ambiente e do Ordenamento do Território, 2013). A large proportion of the area (above 40%) is covered by forestry systems (Autoridade Florestal Nacional and Ministério da Agricultura do Desenvolvimento Rural e das Pescas, 2010) providing a high economical value to the region and the country (Sarmento and Dores, 2013).

2.2 Kernel Density estimation of GDV

Presence datasets of *Quercus suber*, *Quercus ilex* and *Pinus pinea* of the last Portuguese forest inventory achieved in 2010 (ICNF, 2013) were used to calculate Kernel density (commonly called heat map) as a proxy for GDV suitability. Only data points with one of the three proxy species selected as primary and secondary occupation were used. The resulting Kernel density was weighted according to tree cover percentage and was calculated using a quartic biweight distribution shape, a search radius of 10 km, and an output resolution of 0.018 degrees, corresponding to a cell size of 1km. This variable was computed using QGIS version 2.14.12 (QGIS Development Team, 2017).

2.3 Environmental variables

Species distribution is mostly affected by limiting factors controlling ecophysiological responses, disturbances and resources (Guisan and Thuiller, 2005). To characterize the study area in terms of GDV's suitability, environmental variables expected to affect GDV's density were selected according to their constraint on groundwater uptake and soil water storage. Within possible abiotic variables, landscape topography, geology, groundwater availability and regional climate were considered to map GDV density. The twelve selected variables for modeling purposes, retrieved from different data sources are listed in Table 1. The softwares used in spatial analysis were ArcGIS® software version 10.4.1 by Esri and R program software version 3.4.2 (R Development Core Team, 2016).

2.3.1 Slope and soil characteristics

The NASA and METI ASTER GDEM product was retrieved from the online Data Pool, courtesy of the NASA Land Processes Distributed Active Archive Center (LP DAAC), USGS/Earth Resources

Observation and Science (EROS) Center, Sioux Falls, South Dakota, https://lpdaac.usgs.gov/data_access/data_pool.. Spatial Analyst Toolbox was used to calculate the slope from the digital elevation model. Slope was used as proxy for the identification of shallow soil water interaction with vegetation.

The map of soil type was obtained from the Portuguese National Information System for the Environment - SNIAmb (© Agência Portuguesa do Ambiente, I.P., 2017) and uniformized to the World Reference Base with the Harmonized World Soil Database v 1.2 (FAO et al., 2009). The vector map was converted to raster using the Conversion Toolbox. To reduce the analysis complexity involving the several soil types present in the map, soil types were regrouped in three classes, according to their capacity to store or drain water (Table A1 in appendix A). The classification was based on the characteristics of each soil unit (available water storage capacity, drainage and topsoil texture) from the Harmonized World Soil Database (FAO et al., 2009). In the presence of dominant soil with little drainage capacity, AWC and mainly topsoil clay fraction, lower scores were given to higher shallow soil water retention and decreased suitability for GDV. Otherwise, when soil characteristics suggested water storage at deeper soil depths, lower AWC, drainage and sand topsoil texture, higher scores were given.

Effective soil thickness (Table 1) was also considered for representing the maximum soil depth explored by the vegetation roots. It constrains the expansion and growth of the root system, as well as the available amount of water that can be absorbed by roots.

2.3.2 Groundwater availability

Root access to water resources is one of the most limiting factors for GDV's growth and survival, especially during the dry season. The map of depth to water table was interpolated from piezometric observations from the Portuguese National Information System on Water Resources (SNIRH) public data base (http://snirh.apambiente.pt, last accessed on March 31st 2017) and the Study of Groundwater Resources of Alentejo (ERHSA) (Chambel et al., 2007). Data points of large-diameter wells and piezometers were retrieved for the Alentejo region (fig02) and sorted into undifferentiated, karst or porous geological types to model groundwater depth (GWDepth). In the studied area, piezometers are exclusively dedicated structures for piezometric observations, in areas with high abstraction volumes for public water supply. Oppositely, large wells are mainly devoted to private use and low volume abstractions. Due to the large heterogeneity of geological media, groundwater depth was calculated separately for each sub-basin. A total of 3158 data points corresponding to large wells and piezometers were used, with uneven measurements between 1979 and 2017. For each piezometer an average depth was calculated from the available observations and used as a single value. In areas with undifferentiated geological type, piezometric level and elevation were highly correlated (>0.9), thus a linear regression was applied to interpolate data. Ordinary kriging was preferred for the interpolation of karst and porous aquifers, combining large wells and piezometric data points. To build a surface layer of the depth to water table, the interpolated surface of the groundwater level was subtracted from the digital elevation model. Geostatistical Analyst ToolBox was used for this task.

Drainage density is a measure of how well the basin is drained by stream channels. It is defined as the total length of channels per unit area. Drainage density was calculated for a 10km grid size for the Alentejo region, by the division of the 10km square area (A) in km^2 by the total stream length (L) in km, as in Eq. (1).

$$Dd = \frac{L}{A}, \quad (1)$$

2.3.3 Regional Climate

Temperature and precipitation datasets were obtained from the E-OBS (http://eca.knmi.nl/download/ensembles/ensembles.php, last accessed on March 31st 2017) public database (Haylock et al., 2008). Standardized Precipitation Evapotranspiration Index (SPEI), Aridity Index (AI) and Ombrothermic Indexes were computed from long-term (1951-2010) monthly temperature and precipitation observations. The computation of potential evapotranspiration (PET) was performed according to Thornthwaite (1948) and was assessed using the SPEI package (Beguería and Vicente-Serrano, 2013) in R program.

SPEI multi-scalar drought index (Vicente-Serrano et al., 2010) was calculated over a 6 month interval to characterize drought severity in the area of study using SPEI package (Beguería and Vicente-Serrano, 2013) for R program. SPEI is based on the normalization of the water balance calculated as the difference between cumulative precipitation and PET for a given period at monthly intervals. Normalized values of SPEI typically range between -3 and 3. Drought events were considered as severe when SPEI values were between -1.5 and -1.99, and as extreme with values below -2 (Mckee et al., 1993). Severe and extreme SPEI predictors were computed as the number of months with severe or extreme drought, counted along the 60 years of the climate time-series.

While the SPEI index used in this study identifies geographical areas affected with more frequent extreme droughts, the Aridity index (AI) distinguishes arid geographical areas prone to annual negative water balance (with low AI value) to more mesic areas showing positive annual water balance (with high AI value). AI gives information related to evapotranspiration processes and rainfall deficit for potential vegetative growth. It was calculated following Eq. (2) according to Middleton et al. (1992), where PET is the average annual potential evapotranspiration and P is the average annual precipitation, both in mm for the 60 years period of the climate time-series. Dry lands are defined by their degree of aridity in 4 classes: Hyperarid (AI<0.05); Arid (0.05<AI<0.2); Semi-arid (0.2<AI<0.5) and Dry Subhumid (0.5<AI<0.65) (Middleton et al., 1992).

$$AI = \frac{P}{PET}, \quad (2)$$

Ombrothermic Indexes were used to better characterize the bioclimatology of the study region (Rivas-Martínez et al., 2011), by evaluating soil water availability for plants during the driest months of the year. Four ombrothermic indexes were calculated according to a specific section of the year stated in Table 1, and following Eq. (3), where Pp is the positive annual precipitation (accumulated monthly precipitation when the average monthly mean temperature is higher than 0°C) and Tp is the positive annual temperature (total in tenths of degrees centigrade of the average monthly temperatures higher than 0°). Ombrothermic index presenting values below 2 for the analyzed months, can be considered as Mediterranean bioclimatically. For non-Mediterranean areas, there is no dry period in which, for at least two consecutive months, the precipitation is less than or equal to twice the temperature.

$$Io = \frac{Pp}{Tp}, \qquad (3)$$

2.4 Model predictors selection

The full set of environmental variables was evaluated as potential predictors for the suitability of GDV (based on the Kernel density of the proxy species). A preliminary selection was carried out, first by computing Pearson's correlation coefficients between environmental variables and second by performing a Principal Components Analysis (PCA) to detect multicollinearity. Covariates were discarded for modeling according to a sequential procedure. Whenever pairs of variables presented a correlation value above 0.4, the variable with the highest explained variance on the first axis of the PCA was selected. In addition, selected variables had to show the lowest possible correlation values between them. Variables showing low correlations and explaining a higher cumulative proportion of variability with the lowest number of PCA axis were later selected as predictors for modeling. PCA was performed using the GeoDa Software (Anselin et al., 2006) and Pearson's correlation coefficients were computed with Spatial Analyst Tool .

2.5 Model development

When fitting a linear regression model based on the selected variables, the normal distribution and stationarity of the model predictors and residuals must be assured.

The Kernel density of the proxy GDV species, *Q. suber*, *Q. ilex* and *P. pinea,* showed a skewed normal distribution. Therefore, a square-root normalization of the data was applied on this response variable, before model fitting. To be able to compare the resulting model coefficients and use them as weighting factors of the multi-criteria analysis to build the suitability map, the predictor variables were normalized using the z-score function. This allows to create standardized scores for each variable, by subtracting the mean of all data points from each individual data point, then dividing those points by the standard deviation of all points, so that the mean of each z-predictor is zero and the deviation is 1.

Spatial autocorrelation and non-stationarity are common when using linear regression on spatial data. To overcome these issues, Geographically Weighted Regression (GWR) was used to allow model coefficients to adjust to each location of the dataset, based on the proximity of sampling locations (Stewart Fotheringham et al., 1996). In this study, simple linear regression and GWR were both applied to the dataset and their performances compared. Models were fitted on a 5% random subsample of the entire dataset (6242 data points), due to computational restrictions and to decrease the spatial autocorrelation effect (Kühn, 2007). This methodology has already been applied with a subsample of 10%, with points distant 10km from each other (Bertrand et al., 2016). In our dataset, even though we selected a 5% subsample, the mean and maximum distance between two random data points were, respectively, 3.6 km and 16.7 km, providing a good representation of local heterogeneity, as shown in figures 05 and 06. An additional analysis showing an excellent agreement between the two datasets is presented in FigA1 in appendix A.

Initially the model was constructed containing all selected predictors through the PCA and Pearson's correlation analysis. After, we sequentially discarded predictors so as to ascertain the model presenting lower second-order Akaike Information Criteria (AICc) and higher quasi-global R^2 chosen to predict the suitability of GDV.

Adaptive Kernel bandwidths for the GWR model fitting were used due to the spatial irregularity of the random subsample. Bandwidths were obtained by minimizing the CrossValidation score (Bivand et al., 2008). To analyze the performance of the GWR model alone, the local and global adjusted R-squared were considered. To compare between the GWR model and the simple linear model, we considered the distribution of the model residuals, e.g. whether there were visible clustered values and the AICc. The spatial autocorrelation of the models residuals was evaluated with the Moran's I test (Moran, 1950) using the Spatial Statistics Tool, and also graphically. GWR model was fitted using the *spgwr* package from R program (Bivand and Yu, 2017).

2.6 Suitability map building

To create the suitability map we proceeded with the classification of all predictor layers included in the GWR model, similarly to Condesso de Melo et al. (2015) and Aksoy et al. (2017) . The likelihood of an interaction between the vegetation and groundwater resources was scored from 1 to 3 for each predictor. Scores were assigned after bibliographic review and expert opinion. The higher the score, the higher the likelihood, 1 corresponding to a weak likelihood and 3 indicating very high likelihood. Groundwater depth was divided in two classes, according to the accessibility to shallow soil water above 1.5 m and the maximum rooting depth for Mediterranean woody species reaching 13 m, reported by Canadell et al. (1996). Throughout the manuscript, we designated as shallow soil water the water between 0 and 1.5 m depth, while water below 1.5 m depth was considered as groundwater. The depth class between 0 and 1.5m was based on the riparian vegetation in semi-arid Mediterranean areas which is mainly composed of shrub communities (Salinas et al., 2000) and present a mean rooting depths of 1.5m (Silva and Rego, 2004). The most common tree species rooting depth in riparian ecosystems is normally similar to the depth of fine sediment not reaching gravel substrates (Singer et al., 2012) and not reaching levels as deep as deep-rooted species. The minimum score was given to areas where groundwater depth was too shallow (below 1.5 m) considered to belong to surface groundwater dependent vegetation. Areas with steep slope were considered to have superficial runoff and less recharge and influence negatively tree density (Costa et al., 2008). Those areas were treated as less suitable to GDV. Values of the Ombrothermic Index of the summer quarter and the immediately previous month (Ios4) were split in 3 classes according to Jenks natural breaks, with higher suitability corresponding to higher aridity. The higher values of AI, corresponding to lower aridity had a score of 1, because a higher humid environment would decrease the necessity of the arboreous species to use deep water sources. Accordingly, an increase in aridity (lower values of AI) has already been shown to increase tree decline (Waroux and Lambin, 2012) and so higher AI values corresponded to a score of 2, leaving the score 3 to intermediate values of AI. Drainage density scoring was based on the capability of drainage of the water through the hydrographical network of the river. When drainage density was lower (below 0.5), a higher suitability scoring was given because the water lost from runoff through the hydrographic network would be less available to the vegetation thus favoring a higher use of water from groundwater reservoirs (Rodrigues, 2011).

A direct compilation of the predictor layers could have been performed for the multicriteria analysis. However some predictors might have a stronger influence on the GEV distribution and density than others. Therefore, there was a need to define weighting factors for each layer of the final GIS multicriteria analysis. Yet, due to the intricate relations between all environmental predictors and their effects on the GDV, experts and stakeholders suggested very different scoring for a same layer. Subsequently, we instead chose to use the relative proportion of each predictor's coefficient locally, according to the GWR model (Eq. 4) as weighting factors. The final GIS multicriteria analysis was performed using the Spatial Analyst Tool by applying local model equations obtained for each of the 6242 coordinates of the Alentejo map (Eq.4),

$$Suitability = Intercept + coef_1 * [real\ value\ X_1] + coef_2 * [real\ value\ X_2] + coef_3 * [real\ value\ X_3] + \ldots, \quad (4)$$

with brackets representing the reclassified GIS X layer corresponding to the scoring and $coef_{px}$ indicating the relative proportion for the predictor *x*.

According to this equation, lower values indicate a lower occurrence of groundwater use referred a lower GDV suitability while higher values correspond to a higher use of groundwater referred a higher GDV suitability. To allow for an easier interpretation, the data on suitability to GDV was subsequently classified based on their distribution value, according to Jenks natural breaks. This resulted in 5 suitability classes: "Very poor", "Poor", "Moderate", "Good" and "Very Good".

2.7 Map validation

The Normalized Difference Water Index (NDWI) (Gao, 1996) is a satellite-derived index estimating the leaf water content at canopy level, widely used for drought monitoring (Anderson et al., 2010, Gu et al., 2007; Ceccato et al., 2002a) and to estimate fuel moisture content (Maki et al., 2004). NDWI is computed using the near infrared (NIR) and the short-wave infrared (SWIR) reflectance, which makes it sensitive to changes in liquid water content and in vegetation canopies (Gao, 1996; Ceccato et al., 2002a,b). NDWI computation (Eq. X) was further adapted by Gond et al. (2004) to SPOT-VEGETATION instrument datasets, using NIR (0.84 µm) and MIR (1.64 µm) channels, as described by Hagolle et al. (2005).

$$NDWI = \frac{\rho_{NIR} - \rho_{MIR}}{\rho_{NIR} + \rho_{MIR}}. \quad (5)$$

Following Eq. (5), NDWI data were computed using B3 and MIR data acquired from VEGETATION instrument on board of SPOT4 and SPOT5 satellites. Extraction and corrections procedures applied to optimize NDWI series are fully described in Gouveia et al. (2009 and 2012).

The NDWI anomaly was computed as the difference between NDWI observed in June, July and August of 2005 and the median NDWI for the same month for the period 1999 to 2009. June was selected to provide the best signal from a still fully active canopy of woody species while the herbaceous layer had usually already finished its annual cycle and dried out. The hydrological year of 2004/2005 was characterized by an extreme drought event over the Iberian Peninsula, where less than 40% of the normal precipitation was registered in the southern area (Gouveia et al., 2009). Thus, in June 2005 the vegetation of the Alentejo region was already coping with an extreme long-term drought, which was well captured by the anomaly of the NDWI index, as shown by Gouveia et al. 2012.

3 Results

3.1 Kernel Density

Within the studied region of Portugal, the phreatophyte species *Quercus suber, Quercus ilex* and the suspected phreatophyte species *Pinus pinea* were not distributed uniformly throughout the territory. Areas with higher Kernel density (or higher distribution likelihood) were mostly spread between the northern part of Alentejo region and the western part close to the coast, with values ranging between 900 and 1200 (fig03). Two clusters of high density also appeared below the Tagus river. The remaining study area presented mean density values, with a very low density in the area of the river Tagus.

3.2 Environmental conditions

The exploratory analysis of the variables, performed through the PCA and Pearson correlation matrix confirmed the presence of multicollinearity. From the initial variables (Table 1), Thickness, Spei_severe, Spei_extreme, Annual Ombrothermic Index (Io), Ombrothermic Index of the hottest month of the summer quarter(Ios1) and Ombrothermic Index of the summer quarter **(**Ios3) were discarded, while the variables slope, drainage density, soil type, groundwater depth, AI and Ios4 were maintained for analysis (figA2 and Table A1 in appendix). A sequential removal of each predictor from the model with the six variables was performed (table 2) which allowed to choose the model with the highest global R^2 (0.99) and the lowest AICc (18050.34). Therefore, five environmental variables out of the initial 12 considered (fig04) were endorsed to explain the variation of the Kernel density of GDV in Alentejo: AI, Ios4, GWDepth, Dd and slope.

In most part of the Alentejo region, slope was below 10% (fig04e) andcoastal areas presenting the lowest values and variability. Highest values of groundwater depth (fig04c), reaching a maximum of 255 m, were found in the Atlantic margin of the study area, mainly in Tagus and Sado river basins. Several other small and confined areas in Alentejo also showed high values, corresponding to aquifers of porous or karst geological types. Most of the remaining study area showed groundwater depths ranging between 1.5 m and 15 m. Figures 04a and 04b indicate the southeast of Alentejo as the driest area, given by minimum values of the aridity index (0.618), and potential evapotranspiration much higher that precipitation. Besides, Ios4 presented a maximum value (0.714) for this region (meaning that soil water availability was not compensated by the precipitation of the previous M-J-J-A months). This is also supported by the higher drainage density in the southeast which indicates a lower prevalence of shallow soil water due to higher stream length by area.

Combining all variables, it was possible to distinguish two sub-regions with distinct conditions: the southeast of Alentejo and the Atlantic margin. The latter is mainly distinguished by its low slope areas, higher groundwater depth and more humid climatic conditions than the southeast of Alentejo.

3.3 Regression models

The best model to describe the GDV distribution was found through a sequentially discard of each variable (Table 2) and corresponded to the model with a distinct lower AICc (18050.76) compared with the second lowest AICc (27389.74) and showed an important increase in quasi-global R^2 (from 0.926 for the second best model to 0.992 for the best one). The best model fit was obtained with AI, Ios4, GWDepth, Dd and slope. This final model was then applied to the GIS layers to map the suitability of GDV in Alentejo, according to Eq. 6.

$$Suitability = Intercept + AI\ coef_p * [reclassified\ AI\ value] + Ios4\ coef_p * [reclassified\ Ios4\ value] + GWDepth\ coef_p * [reclassified\ GWDepth\ value] + Dd\ coef_p * [reclassified\ Dd\ value] + slope\ coef_p * [reclassified\ slope\ value], \quad (6)$$

Local adjusted R-squared of the GWR model was highly variable throughout the study area, ranging from 0 to 0.99 (fig05). Also, the local R-squared values below 0.5 corresponded to only 0.3% of the data. The lower R-squared values were distributed throughout the Alentejo area, with no distinct pattern. The overall fit of the GWR model was high (Table 3). The adjusted regression coefficient indicated that 99% of the variation in the data was explained by the GWR model, while only 0.02% was explained by the simple linear model (Table 3). Accordingly, GWR had a substantially lower AICc when compared with the simple linear model, indicating a much better fit.

The spatial autocorrelation given by the Moran Index (Griffith, 2009; Moran 1950) retrieved from the geospatial distribution of residual values was significant for both GWR and linear model. It was substantially lower for the GWR model though, than for the linear model (-z-score of 50.24 and 147.56 respectively). Indeed, in the linear model (fig06b), positive residuals were condensed in the right side of Tagus and Sado river basins, while negative values were mainly present on the left side of the Tagus river and in the center-south of Alentejo. In the GWR model (fig06a) the positive and negative residual values were much more randomly scattered throughout the study region, highlighting a much better performance of the GWR, which minimized residual autocorrelation.

The spatial distribution of the coefficients of GWR predictors are presented in Fig07. They were later used for the computation of the GDV suitability score for each data point (Eq.6). The coefficient variability was three times higher for the Aridity Index as compared to Ios4 (fig08), reaching 66 and 22% respectively. For GWDepth, Dd and Slope, the coefficient variation was much lower, representing only about 6.2, 3.8 and 1.2% of the total variation observed in the coefficients, respectively. The remaining variables showed a median close to 0 and the Ios4 was the second with higher variability followed by the GWDepth. The coefficient median values were, respectively, -3.40, 0.29, -0.015, -0.018 and 0.022 for AI, Ios4, GWDepth, Dd and Slope variables.

The distributions of negative coefficients were similar for AI and the Ios4 variables (fig07a and fig07b), with lower values in the southern coastal area, and in the Tagus river watershed. The highest absolute values were mostly found for AI in the southern area of the Alentejo region and on smaller patches in the northern region. In the center and easter areas of Alentejo a higher weight of the groundwater depth coefficient could be found (fig07c), approximately matching a higher influence of slope (fig07e). The GWDepth seemed to have almost no influence on GDV density in the Tagus river watershed, expressed by coefficients mostly null around the riverbed (fig07c). The coefficient distribution of Dd and Ios4 shows some similarities, mostly in the center and southeats of Alentejo (fig07d). Extreme values of Ios4 coefficients were mostly concentrated in the eastern part of the Tagus watershed and in the southern coastal area included in the Sado watershed. Slope coefficient values showed the lowest amplitude throughout the study area (fig07e), with prevailing high positive values gathered mainly in the center of the study area and in the Tagus river watershed (northwest of the study center).

3.4 GDV Suitability map

The classification of the 5 endorsed environmental predictors is presented in Table 4 and their respective maps in figure B1 in appendix B. Rivers Tagus and Sado had an overall positive impact on GDV's suitability for each predictor, with the exception of AI and GWDepth. This is due to a higher water availability reflected by the values of the Ios4, the Dd and the lower slopes due to the alluvial plains of the Tagus river (figs. B1b,d and e in appendix B). On the other hand, those regions also presented higher humidity conditions (through analysis of the AI in fig B1a in appendix B) and groundwater depths outside the optimum range (Fig. B1c in appendix B), therefore less suitable for GDV. Optimal conditions for groundwater access were mainly gathered in the interior of the study region (fig. B1c in appendix B), with the exception of some confined aquifers in the northeast and southeast of the study region. Favorable slopes for GDV were mostly highlighted in the Tagus river basin area, where a good likelihood of interaction between GDV and groundwater could be identified (fig. B1e in appendix B).

The final map illustrating the suitability to GDV is shown in Fig. 09. The proportion of each suitability class was quite evenly distributed throughout the study area. The largest area (8 787km^2) presented a very poor suitability to GDV but corresponded only to approximately a quarter of the total study area (0.29%). This percentage was followed closely by the moderate suitability to GDV which occupied 0.26% (8000km^2). Overall, the two less suitable classes (very poor and poor) represented 0.47% of the study area, whilst the two best ones and the moderate class (very good, good and moderate) represented 0.53%. Consequently, most of the study area showed high to moderate suitability to GDV. The very good and good suitability classes corresponded to the most southern and eastern center area of the Alentejo region, mainly close to the coastal line, passing through the Sado Guadiana river basins. Most of the center of the study area showed moderate to very good suitability do GDV, while the areas corresponding to the alluvial deposits of the Tagus river showed poor to very poor suitability.

The suitability to GDV in the Alentejo region was mainly driven by the AI, given by the highest coefficient variability associated to the AI predictor in the GWR model equation. This is also supported by the similar distribution pattern observed between the suitability map and the aridity index predictor (fig04a and fig09). Areas with good or very good suitability mostly matched areas of AI with score 3 (Fig. B1a in appendix B). On the other hand, the lowest suitability classes showed a good agreement with the lowest scores given to GWDepth (Fig. B1c in appendix B), mostly in the coastal area and in the Tagus river basin.

3.5 Map validation

To assess the accuracy of the suitability map developed in the present study, we compared our results with the NDWI anomaly considering the month of June of the dry year of 2005 in the Alentejo area (fig10). Both maps (figs 09 and 10) showed similar areas for higher and lower presence for GDV. The NDWI anomaly was mostly negative over the Alentejo territory indicating water stress in the vegetation leaves. Water stress due to the extreme drought was maximum (brown colour) in geographical areas matching the highest GDV suitability (fig09). It was less pronounced (mostly yellowish) in the central area of the Alentejo region between the Guadiana and Sado river basins where the vegetation presents a lower density (fig03). Areas with positive/null values of NDWI anomaly (corresponding to a higher water availability) were mostly distributed on the coastal area of the Atlantic ocean or close to riverbeds, namely in the Tagus and Sado floodplains (green colour, fig10), matching areas of poor suitability for GDV in Figure 09.

4 Discussion

4.1 Modeling approach

The Geographically Weighted Regression model has been used before in ecological studies (Li et al., 2016; Mazziotta et al., 2016), but never for the mapping of GDV, to our knowledge. This approach considerably improved the goodness of fit when compared to the linear model, with a coefficient of regression (R^2) increasing from 0.02 to 0.99 at the global level, and an obvious reduction of residual clustering. Despite those improvements, it has not been possible to completely eliminate the residual autocorrelation after fitting the GWR model.

Kernel density for the study area provided a strong indication of presence and abundance of the tree species considered as GDV proxy for modeling. Mediterranean cork woodlands (Montados) are agroforestry systems considered as semi-natural ecosystems, that must be continually maintained through human management by thinning, understory use through grazing, ploughing and shrub clearing (Huntsinger and Bartolome, 1992) to maintain a good productivity, biodiversity and ecosystems service (Bugalho et al., 2009). Montados dominate about 76% of the Alentejo region (while only 7% is covered by stone pine). In those systems, tree density is known to be a tradeoff between climate drivers (Joffre 1999, Gouveia & Freitas 2008) and the need for space for pasture or cereal cultivation in the understory (Acacio & Holmgreen 2014). In our study, the anthropologic management of agroforestry systems in the Alentejo region has not been taken into account. This could, at least partially, explain the non-randomness of the residual distribution after GWR model fitting as well as the mismatches between the GDV and the validation maps.

Another explanation of the reminiscent autocorrelation after GWR fitting could be the lack of groundwater dependent species in the model. For example, we decided to exclude *Pinus pinaster* Aiton due to its more humid distribution in Portugal, and due to conflicting conclusions driven from previous studies to pinpoint the species as a potential groundwater user (Bourke, 2004; Kurz-Besson et al., 2016). In addition, we excluded olive trees although the use of groundwater by an olive orchard has been recently proved (Ferreira et al., 2018), however with a weak contribution of groundwater to the daily root flow, and thus with no significant impact of groundwater on the species physiological conditions.

Methods previously used by Doody et al., (2017) and Condesso de Melo et al. (2015) to map specific vegetation relied solely on expert opinion, e.g. Delphi panel, to define weighting factors of environmental information for GIS multicriteria analysis. In our study, we used a GWR modelling approach to assess weighting factors for each environmental predictor in the study area, to build a suitability map for the GDV in southern Portugal. This allowed an empirical determination of the local relevance of each environmental predictor in GDV distribution, thus avoiding the inevitable subjectivity of Delphi panels. Modelling of the entire study region at a regional level did not provide satisfactory results. Therefore, we developed a general model varying locally according to local predictor coefficients. The local influence of each predictor was highly variable throughout the study area, especially for climatic predictors reflecting water availability and stress conditions. The application of the GWR model did not only allowed for a localized approach, by decreasing the residual error and autocorrelation over the entire studied region, but also provided insights on how GDV's density can be explained by the main environmental drivers locally.

Predictor coefficients showed a similar behavior in the spatial distribution of the coefficients. This was noticeable for the aridity index and the groundwater depth in the Tagus and Sado river basins. Groundwater depth had no influence on GDV's density in these areas and similarly, the coefficient of Aridity index showed a negative effect of increased humidity on GDV's density. In addition, a cluster of low drainage density values matched these areas.

4.2 Suitability to Groundwater Dependent Vegetation

According to our results, more than half of the study area appears suitable for GDV. However, one quarter of the studied area showed the lowest suitability to GDV. The lower suitability to this vegetation in the more northern and western part of the studied area can be explained by less favorable climatic and hydrological conditions, resulting from the combination of a high aridity index and low groundwater depth scores (equivalent to high shallow soil water availability), corresponding to the coastal area and in the Tagus river basin.

Zomer et al. (2009) attempted to quantify the extent of agroforestry at the global level by performing a geospatial analysis of remote sensing derived global datasets. They showed that the average tree cover density within agricultural land can were closely linked to aridity with similar trends for different geographical areas. Our results agree with these findings since the aridity and ombrothermic indexes were the most important predictors of GDV density in the Alentejo region, according to our model outcomes. This is in agreement with former studies linking tree cover/density of Mediterranean oak woodland to climate drivers derived from precipitation (Gouveia and Freitas 2008, Joffre et al. 1999). Also, Waroux and Lambin (2012) studied the degradation of the argania woodlands in semi-arid to arid Southwest Morocco and found that a 44% decline of the forest density was mostly driven by the increasing aridity in the region between 1970 and 2007. Similarly, many studies carried out on oak woodlands in Italy and Spain identified drought as the main driving factor of tree die-back and as the main climate warning threatening oak stands sustainability in the Mediterranean basin (Gentilesca et al. 2017). Tree mortality linked to increasing drought stresses can also be associated to a geographical shift in vegetation communities (Lloret et al., 2004). For example, xeric plant species Sahel have expanded in the north of Sahel since the last half of the 20th century, toward areas of higher rainfall at an average rate of 500 to 600 m yr^{-1} (Gonçalez P., 2001).

In environments with scarce water sources such as the Mediterranean basin, plants have developed strategies to either avoid or escape drought stress (Chaves et al., 2003). The development of a dimorphic root systems in woody species is an adaptation strategy to escape drougth (Dinis 2014, David et al., 2013). When comparing different water limited ecosystems from a global dataset, Schenk and Jackson

(2002) showed that rooting depth increased with aridity. Furthermore, a clear relationship between rooting depth and the water table depth was evidenced at global scale (Fan et al. 2017).

In our study, groundwater depth appeared to have a lower influence on GDV density than climate drivers, as reflected by the relative low magnitude of the GWDepth coefficient in our model outcomes. This surprisingly disagrees with our initial hypothesis because groundwater represents a notable proportion of the transpired water of deep-rooting phreatophytes, reaching up to 86% of absorbed water during drought periods and representing about 30.5% of the annual water absorbed by trees (David et al. 2013, Kurz-Besson et al. 2014). Nonetheless, this disagreement should be regarded cautiously due to the poor quality of the data used. On one hand, data points in the study region were highly heterogeneous, and certain areas showed a better statistical representation than others. Moreover, the high variability in geological media, topography and vegetation cover at the regional scale did not allow to account for small changes in groundwater depth (<15 m deep), which has a huge impact on GDV suitability (Canadell et al., 1996; Stone and Kalisz, 1991). Indeed, a high spatial resolution of hydrological database is essential to rigorously characterize the spatial dynamics of groundwater depth between hydrographic basins (Lorenzo-Lacruz et al., 2017). However, such resolution was not available for our study area. In addition, the lack of temporal data hampered the calculation of seasonal trends in groundwater depth, which are essential under Mediterranean conditions to build a reliable interpolation of observed data. Temporal data would also further help discriminate areas of optimal suitability to GDV, either during the wet and the dry seasons. Investigations efforts should be invested to fill the gap either by improving the Portuguese piezometric monitoring network, or by assimilating observations with remote sensing products focused on soil moisture or groundwater monitoring. This has already been performed for large regional scale such as GRACE satellite surveys, based on changes of Earth's gravitational field. So far, these technologies are not applicable to Portugal's scale, since the coarse spatial resolution of GRACE data only allows the monitoring of large reservoirs (Xiao et al. 2015).

4.4 Validation of the results

Satellite derived remote-sensing products have been widely used to follow the impact of drought on land cover and the vegetation dynamics (AghaKouchaket al. 2015). Vegetation indexes offer excellent tools to assess and monitor plant changes and water stress (Asrar et al. 1989).

The understory of woodlands and the herbaceous layer of grasslands areas in southern Portugal usually ends their annual life cycles in June (Paço et al. 2007), while the canopy of woody species is still fully active with maximum transpiration rates and photosynthetic activities (Kurz-Besson et al. 2014, David et al. 2007, Awada et al. 2003). This is an ideal period of the year to spot differential response of the canopy of woody species to extreme droughts events using satellite derived vegetation indexes (Gouveia 2012). In this manuscript we preferred the NDWI index to be more sensitive to canopy water content and a good proxy for water stress status in plants. Moreover, NDWI has been shown to be best related to the greenness of Cork aok woodland's canopy, expressed by the fraction of intercepted photosynthetically active radiation (Cerasoli et al., 2016).

By looking at the map of the NDWI anomaly in June 2005, it appears that the woody canopy showed a strong loss of canopy water in the areas were tree density and GDV suitability were higher (figs03, 09 and 10). This occurred although trees minimized the loss of water in leaves with a strong stomatal limitation in response to drought (Kurz-Besson et al. 2014, Grant et al. 2010). In the most arid area of the region were Holm oak is dominant but tree density is lower, the NDWI anomaly was generally less negative thus showing a lower water stress or higher canopy water content. Holm oak (*Quercus ilex* spp *rotundifolia*) is well known to be the most resilient species to drought conditions in Portugal, due to its capacity to use groundwater and a higher water use efficiency (David et al. 2007). Furthermore, by looking at the dynamics of NDWI anomaly (fig10) we can see that the lower water stress status on the map is progressively spreading from the most arid areas to the milder ones from June to August 2005, despite the intensification of drought conditions. This endorses the idea that trees manage to cope with drought by relying on deeper water sources in response to drought, replenishing leaf water content despite the progression and intensification of drought conditions. Former studies support this statement by showing that groundwater uptake and hydraulic lift were progressively taking place after the onset of drought by promoting the formation of new root reaching deeper soil layers and water sources, typically in July, for cork oak in the Alentejo region (Kurz-Besson et al., 2006, 2014). Root elongation following a declining water table has also been reported in a review on the effect of groundwater fluctuations on Phreatophytic vegetation (Nuamburg et al. 2005).

Our results and the dynamics of NDWI over summer 2005 tend to corroborate the studies of Schenk and Jackson (2002) and Fan et al. (2017), by suggesting a larger/longer dependency of GDV on groundwater with higher aridity. Further investigation needs to be carried on across aridity gradients in Portugal and the Iberian Peninsula to fully validate this statement, though.

Overall, the map of suitability to GDV showed an excellent agreement with the NDWI validation maps. The main areas showing good suitability are mostly matching in both maps. The good agreement between our GDV suitability maps, and validation maps opens the possibility to apply and extend the methodology to larger geographical areas such as the Iberian Peninsula, or the simulation of the impact of climate changes on the distribution of groundwater dependent species in the Mediterranean basin. Simulations of future climate conditions based on RCP4.5 and RCP8.5 emission scenarios (Soares et al., 2015, 2017) predict a significant decrease of precipitation for the Guadiana basin and overall decrease for the southern region of Portugal within 2100. Agroforestry systems relying on groundwater resources, such as cork oak woodlands, may show a decrease in productivity and ecosystem services or even face sustainability failure. An increase in aridity and drought frequency for the Mediterranean (Spinoni et al., 2017) will most probably induce a shift of GDV vegetation toward milder/wetter climates.

4.3 Key limitations

With the methodology applied in this study, weighting factors can be easily evaluated solely from local and regional observations of the studied area. Nonetheless, either the computation of model coefficients or expert opinion to assess weighting factors, require update, and/or environmental data, species distribution and revised expert knowledge (Doody et al., 2017).

The evolution of groundwater depth in response to climate change is difficult to model on a large scale based on piezometric observations because it requires an excellent knowledge of the components and dynamics of water catchments. Therefore, a reliable estimation of the impact of climate change on GDV suitability in southern Portugal could only been performed on small scale studies. However, we showed that groundwater depth was only accounting for about 6% of the coefficient variation in the studied area, against 89% of the variation represented by climate indexes AI and Ios4. Changes in climate conditions only represents part of the water resources shortage issue in the future. Global-scale changes in human populations and economic progresses also rules water demand and supply, especially in arid and semi-arid regions (Vörösmarty et al., 2000). A decrease in useful water resources for human supply can induce an even higher pressure on groundwater resources (Döll, 2009), aggravating the water table drawdown caused by climate change (Ertürk et al., 2014). Therefore, additional updates of the model should include human consumption of groundwater resources, identifying areas of higher population density or intensive farming. Future model updates should also account for the interaction of deep rooting species with the surrounding understory species. In particular, shrubs surviving the drought period, which can benefit from the redistribution of groundwater by deep rooted species (Dawson, 1993; Zou et al., 2005).

5 Conclusions

Our results show a highly dominant contribution of water scarcity (Aridity and Ombrothermic indexes) on the density and suitability of deep-rooted groundwater dependent species. The contribution of groundwater depth was much lower than we initially expected, accounting only for 6% of the total coefficient variation. This might be underestimated however, due to the poor quality of the piezometric network especially in the central area of the studied region.

The current pressure applied by human consumption of water sources has reinforced the concern on the future of economic activities dependent on groundwater resources. To address this issue, several countries have developed national strategies for the adaptation of water sources for Agriculture and Forests against Climate Change, including Portugal (FAO, 2007). In addition, local drought management as long-term adaptation strategy has been one of the proposals of Iglesias et al. (2007) to reduce the climate change impact on groundwater resources in the Mediterranean. The preservation of Mediterranean agroforestry systems, such as cork oak woodlands and the recently associated *P. pinea* species, is of great importance due to their high socioeconomic value and their supply of valuable ecosystem services (Bugalho et al., 2011). Management policies on the long-term should account for groundwater resources monitoring, accompanied by defensive measures to ensure agroforestry systems sustainability and economical income from these Mediterranean ecosystems are not greatly and irreversibly threatened.

Our present study, and novel methodology, provides an important tool to help delineating priority areas of action for species and groundwater management, at regional level, to avoid the decline of productivity and cover density of the agroforestry systems of southern Portugal. This is important to guarantee the sustainability of the economical income for stakeholders linked to the agroforestry sector in that area. Furthermore, mapping vulnerable areas at a small scale (e.g.by hydrological basin), where reliable groundwater depth information is available, should provide further insights for stakeholder to promote local actions to mitigate climate change impact on GDV.

Based on the methodology applied in this work, future predictions on GDV suitability, according to the RCP4.5 and RCP8.5 emission scenarios will be shortly computed, providing guidelines for future management of these ecosystems in the allocation of water resources.

6 Acknowledgements

The authors acknowledge the E-OBS dataset from the EU-FP6 project ENSEMBLES (http://ensembles-eu.metoffice.com) and the data providers in the ECA&D project (http://www.ecad.eu). The authors also wish to acknowledge the ASTER GDEM data product, a courtesy of the NASA Land Processes Distributed Active Archive Center (LP DAAC), USGS/Earth Resources Observation and Science (EROS) Center, Sioux Falls, South Dakota, https://lpdaac.usgs.gov/data_access/data_pool. We are grateful to ICNF for sharing inventory database performed in 2010 in Portugal continental. We also thank Célia Gouveia, Cristina Catita, Ana Russo and Patrícia Páscoa for the advice and helpful comments as well as Ana Bastos for the elaboration of the satellite datasets of the vegetation index NDWI. We are very grateful to Eric Font for the useful insights on soil properties. I Gomes Marques and research activities were supported by the Portuguese National Foundation for Science and Tecnhology (FCT) through the PIEZAGRO project (PTDC/AAG-REC/7046/2014). The authors would like to thank the reviewers and editor for helpful comments and suggestions on an earlier version of the manuscript.

The authors declare that they have no conflict of interest.

References

Acácio V. and Holmgreen M.: Pathways for resilience in Mediterranean cork oak land use systems, Annals of Forest Science, 71, 5-13, doi: 10.1007/s13595-012- 0197-0, 2009

Aghakouchak, A., Farahmand, A., Melton, F. S., Teixeira, J., Anderson, M. C., Wardlow, B. D. and Hain C. R.: Remote sensing of drought: Progress, challenges and opportunities. Reviews of Geophysics, doi: 10.1002/2014RG000456, 2015.

Aksoy, E., Louwagie, G., Gardi, C., Gregor, M., Schröder, C. and Löhnertz, M.: Assessing soil biodiversity potentials in Europe, Sci. Total Environ., 589, 236–249, doi:10.1016/j.scitotenv.2017.02.173, 2017.

Anderson, L. O., Malhi, Y., Aragão, L. E. O. C., Ladle, R., Arai, E., Barbier, N. and Phillips, O.: Remote sensing detection of droughts in Amazonian forest canopies. New Phytologist, 187, 733–750, doi: 10.1111/j.1469-8137.2010.03355.x, 2010.

Anselin, L., Ibnu, S. and Youngihn, K.: GeoDa: An Introduction to Spatial Data Analysis, Geogr. Anal., 38(1), 5–22, 2006.

APA: Plano de Gestão da Região Hidrográfica do Tejo: Parte 2 - Caracterização e Diagnóstico da Região Hidrográfica, n.d.

ARH Alentejo: Plano de Gestão das Bacias Hidrográficas integradas na RH7 - Parte 2, 2012.

ARH Alentejo: Planos de Gestão das Bacias Hidrográficas integradas na RH6 - Parte 2, 2012.

Asrar, G. (Ed.): Estimation of plant-canopy attributes from spectral reflectance measurements, Theory and Applications of Optical Remote Sensing, pp. 252–296, John Wiley, New York, 1989.

Autoridade Florestal Nacional and Ministério da Agricultura do Desenvolvimento Rural e das Pescas: 5o Inventário Florestal Nacional, 2010.

Awada T., Radoglou K., Fotelli M. N., Constantinidou H. I. A.: Ecophysiology of seedlings of three Mediterranean pine species in contrasting light regimes, Tree Physiology, 23, 33–41, 2003.

Barata, L. T., Saavedra, A., Cortez, N. and Varennes, A.: Cartografia da espessura efectiva dos solos de Portugal Continental. LEAF/ISA/ULisboa. [online] Available from: http://epic-webgis-portugal.isa.utl.pt/, 2015.

Barbero, M., Loisel, R. and Quézel, P.: Biogeography, ecology and history of Mediterranean *Quercus ilex* ecosystems, in *Quercus ilex* L. ecosystems: function, dynamics and management, edited by F. Romane and J. Terradas, pp. 19–34, Springer Netherlands, Dordrecht., 1992.

Barbeta, A. and Peñuelas, J.: Increasing carbon discrimination rates and depth of water uptake favor the growth of Mediterranean evergreen trees in the ecotone with temperate deciduous forests, Glob. Chang. Biol., 1–15, doi:10.1111/gcb.13770, 2017.

Barbeta, A., Mejía-Chang, M., Ogaya, R., Voltas, J., Dawson, T. E. and Peñuelas, J.: The combined effects of a long-term experimental drought and an extreme drought on the use of plant-water sources in a Mediterranean forest, Glob. Chang. Biol., 21(3), 1213–1225, doi:10.1111/gcb.12785, 2015.

Barron, O. V., Emelyanova, I., Van Niel, T. G., Pollock, D. and Hodgson, 0G.: Mapping groundwater-dependent ecosystems using remote sensing measures of vegetation and moisture dynamics, Hydrol. Process., 28(2), 372–385, doi:10.1002/hyp.9609, 2014.

Beguería, S. and Vicente-Serrano, S. M.: SPEI: Calculation of the Standardized Precipitation-Evapotranspiration Index. R package version 1.6., 2013.

Bertrand R., Riofrío-Dillon G., Lenoir J., Drapier J., de Ruffray P., Gégout J. C. and Loreau M.: Ecological constraints increase the climatic debt in forests, Nature Communications, 7, 12643, doi: 10.1038/ncomms12643, 2016.

Bivand, R. and Yu, D.: spgwr: Geographically Weighted Regression. [online] Available from: https://cran.r-project.org/package=spgwr, 2017.

Bivand, R. S., Pebesma, E. J. and Gómez-Rubio, V.: Applied Spatial Data Analysis with R, edited by G. P. Robert Gentleman, Kurt Hornik, Springer., 2008.

Bourke, L.: Growth trends and water use efficiency of *Pinus pinaster* Ait. in response to historical climate and groundwater trends on the Gnangara Mound, Western Australia, 2004.

Bugalho, M. N., Plieninger, T. and Aronson, J.: Open woodlands: a diversity of uses (and overuses), in Cork oak woodlands on the edge, edited by J. Aronson, J. S. Pereira, and J. G. Pausas, pp. 33–48, Island Press, Washington DC., 2009.

Bugalho, M. N., Caldeira, M. C., Pereira, J. S., Aronson, J. and Pausas, J. G.: Mediterranean cork oak savannas require human use to sustain biodiversity and ecosystem services, Front. Ecol. Environ., 9(5), 278–286, doi:10.1890/100084, 2011.

Bussotti, F., Ferrini, F., Pollastrini, M. and Fini, A.: The challenge of Mediterranean sclerophyllous vegetation under climate change: From acclimation to adaptation, Environ. Exp. Bot., 103(April), 80–98, doi:10.1016/j.envexpbot.2013.09.013, 2013.

Canadell, J., Jackson, R., Ehleringer, J., Mooney, H. A., Sala, O. E. and Schulze, E.-D.: Maximum rooting depth of vegetation types at the global scale, Oecologia, 108, 583–595, doi:10.1007/BF00329030, 1996.

del Castillo, J., Comas, C., Voltas, J. and Ferrio, J. P.: Dynamics of competition over water in a mixed oak-pine Mediterranean forest: Spatio-temporal and physiological components, For. Ecol. Manage., 382, 214–224, doi:10.1016/j.foreco.2016.10.025, 2016.

Ceccato, P., Gobron, N., Flasse, S., Pinty, B. and Tarantola, S.: Designing a spectral index to estimate vegetation water content from remote sensing data: Part 1. Theoretical approach. Remote Sensing of Environment, 82, 188 – 197, 2002a.

Ceccato, P., Flasse, S. and Gregoire, J.: Designing a spectral index to estimate vegetation water content from remote sensing data: Part 2. Validation and applications. Remote Sensing of Environment, 82, 198 – 207, 2002b.

Centenaro, G., Hudek, C., Zanella, A. and Crivellaro, A.: Root-soil physical and biotic interactions with a focus on tree root systems: A review, Appl. Soil Ecol., doi:10.1016/J.APSOIL.2017.09.017, 2017.

Cerasoli S., Silva F.C. and Silva J. M. N.: Temporal dynamics of spectral bioindicators evidence biological and ecological differences among functional types in a cork oak open woodland, Int J Biometeorol., 60 (6), 813–825, doi: 10.1007/s00484-015-1075-x, 2016.

Chambel, A., Duque, J. and Nascimento, J.: Regional Study of Hard Rock Aquifers in Alentejo, South Portugal: Methodology and Results, in Groundwater in Fractured Rocks - IAH Selected Paper Series, pp. 73–93, CRC Press., 2007.

Chaves M. M., Maroco J. P. and Pereira J.S.: Understanding plant responses to drought — from genes to the whole plant, Funct Plant Biol, 30(3), 239 - 264, 2003.

Coelho, I. S. and Campos, P.: Mixed Cork Oak-Stone Pine Woodlands in the Alentejo Region of Portugal, in Cork Oak Woodlands on the Edge - Ecology, Adaptive Management, and Restoration, edited by J. Aronson, J. S. Pereira, J. Uli, and G. Pausas, pp. 153–159, Island Press, Washington, 2009.

Condesso de Melo, M. T., Nascimento, J., Silva, A. C., Mendes, M. P., Buxo, A. and Ribeiro, L.: Desenvolvimento de uma metodologia e preparação do respetivo guia metodológico para a identificação e caracterização, a nível nacional, dos ecossistemas terrestres dependentes das águas subterrâneas (ETDAS). Relatório de projeto realizado para a Agência Portuguesa do Ambiente, 2015.

Costa, A., Madeira, M. and Oliveira, C.: The relationship between cork oak growth patterns and soil, slope and drainage in a cork oak woodland in Southern Portugal, For. Ecol. Manage., 255, 1525–1535, doi:10.1016/j.foreco.2007.11.008, 2008.

David, T. S., Ferreira, M. I., Cohen, S., Pereira, J. S. and David, J. S.: Constraints on transpiration from an evergreen oak tree in southern Portugal, Agric. For. Meteorol., 122(3–4), 193–205, doi:10.1016/j.agrformet.2003.09.014, 2004.

David, T. S., Henriques, M. O., Kurz-Besson, C., Nunes, J., Valente, F., Vaz, M., Pereira, J. S., Siegwolf, R., Chaves, M. M., Gazarini, L. C. and David, J. S.: Water-use strategies in two co-occurring Mediterranean evergreen oaks: surviving the summer drought., Tree Physiol., 27(6), 793–803, doi:10.1093/treephys/27.6.793, 2007.

David, T. S., Pinto, C. A., Nadezhdina, N., Kurz-Besson, C., Henriques, M. O., Quilhó, T., Cermak, J., Chaves, M. M., Pereira, J. S. and David, J. S.: Root functioning, tree water use and hydraulic redistribution in *Quercus suber* trees: A modeling approach based on root sap flow, For. Ecol. Manage., 307, 136–146, doi:10.1016/j.foreco.2013.07.012, 2013.

Dawson, T. E.: Hydraulic lift and water use by plants: implications for water balance, performance and plant-plant interactions, Oecologia, 95, 565–574, 1993.

Dinis, C.O.: Cork oak (*Quercus suber* L.) root system: a structural-functional 3D approach. PhD Thesis, Universidade de Évora (Portugal), 2014.

Döll, P.: Vulnerability to the impact of climate change on renewable groundwater resources: a global-scale assessment, Environ. Res. Lett., 4(4), 35006–12, doi:10.1088/1748-9326/4/3/035006, 2009.

Doody, T. M., Barron, O. V., Dowsley, K., Emelyanova, I., Fawcett, J., Overton, I. C., Pritchard, J. L., Van Dijk, A. I. J. M. and Warren, G.: Continental mapping of groundwater dependent ecosystems: A methodological framework to integrate diverse data and expert opinion, J. Hydrol. Reg. Stud., 10, 61–81, doi:10.1016/j.ejrh.2017.01.003, 2017.

Dresel, P. E., Clark, R., Cheng, X., Reid, M., Terry, A., Fawcett, J. and Cochrane, D.: Mapping Terrestrial Groundwater Dependent Ecosystems: Method Development and Example Output., 2010.

Duque-Lazo, J., Navarro-Cerrillo, R. M. and Ruíz-Gómez, F. J.: Assessment of the future stability of cork oak (*Quercus suber* L.) afforestation under climate change scenarios in Southwest Spain, For. Ecol. Manage., 409(June 2017), 444–456, doi:10.1016/j.foreco.2017.11.042, 2018.

Eamus, D., Froend, R., Loomes, R., Hose, G. and Murray, B.: A functional methodology for determining the groundwater regime needed to maintain the health of groundwater-dependent vegetation, Aust. J. Bot., 54(2), 97–114, doi:10.1071/BT05031, 2006.

Eamus, D., Zolfaghar, S., Villalobos-Vega, R., Cleverly, J. and Huete, A.: Groundwater-dependent ecosystems: Recent insights from satellite and field-based studies, Hydrol. Earth Syst. Sci., 19(10), 4229–4256, doi:10.5194/hess-19-4229-2015, 2015.

Ertürk, A., Ekdal, A., Gürel, M., Karakaya, N., Guzel, C. and Gönenç, E.: Evaluating the impact of climate change on groundwater resources in a small Mediterranean watershed, Sci. Total Environ., 499, 437–447, doi:10.1016/j.scitotenv.2014.07.001, 2014.

Evaristo, J. and McDonnell, J. J.: Prevalence and magnitude of groundwater use by vegetation: a global stable isotope meta-analysis, Sci. Rep., 7, 44110, doi:10.1038/srep44110, 2017.

Fan Y., Macho G. M., Jobbágy E. G., Jackson R. B. and Otero-Casal C.: Hydrologic regulation of plant rooting depth. Proc. Natl Acad. Sci. USA 114, 10 572–10 577, doi: 10.1073/pnas.1712381114, 2017.

FAO: Adaptation to climate change in agriculture, forestry and fisheries: Perspective, framework and priorities, Rome, 2007.

FAO, IIASA, ISRIC, ISS-CAS and JRC: Harmonized World Soil Database (version 1.1), 2009.

Fernandes, N. P.: Ecossistemas Dependentes de Água Subterranea no Algarve - Contributo para a sua Identificação e Caracterização, University of Algarve., 2013.

Ferreira, M. I., Green, S., Conceição, N. and Fernández, J.-E.: Assessing hydraulic redistribution with the compensated average gradient heat-pulse method on rain-fed olive trees, Plant Soil, 1–21, doi:10.1007/s11104-018-3585-x, 2018.

Filella, I. and Peñuelas, J.: Indications of hydraulic lift by *Pinus halepensis* and its effects on the water relations of neighbour shrubs, Biol. Plant., 47(2), 209–214, doi:10.1023/B:BIOP.0000022253.08474.fd, 2004.

Gao, B.C.: NDWI - A normalized difference water index for remote sensing of vegetation liquid water from space. Remote Sensing of Environment, 58, 257-266, 1996.

Gentilesca T., Camarero J. J., Colangelo M., Nolè A. and Ripullone F.: Drought-induced oak decline in the western Mediterranean region: an overview on current evidences, mechanisms and management options to improve forest resilience, iForest, 10, 796-806, doi: 10.3832/ifor2317-010, 2017.

Giorgi, F. and Lionello, P.: Climate change projections for the Mediterranean region, Glob. Planet. Change, 63(2–3), 90–104, doi:10.1016/j.gloplacha.2007.09.005, 2008.

Gond, V., Bartholome, E., Ouattara, F., Nonguierma, A. and Bado, L. Surveillance et cartographie des plans d'eau et des zones humides et inondables en regions arides avec l'instrument VEGETATION embarqué sur SPOT-4, Int. J. Remote Sens, 25, 987–1004, 2004.

Gonzalez, P.: Desertification and a shift of forest species in the West African Sahel, Clim. Res., 17, 217–228, 2001.

Gouveia A. and Freitas H.: Intraspecific competition and water use efficiency in *Quercus suber*: evidence of an optimum tree density?, Trees, 22, 521-530, 2008.

Gouveia C., Trigo R. M., DaCamara C. C.: Drought and Vegetation Stress Monitoring in Portugal using Satellite Data, Nat Hazards Earth Syst Sci, 9, 1-11, doi: 10.5194/nhess-9-185-2009, 2009.

Gouveia C. M., Bastos A., Trigo R. M., DaCamara C. C.: Drought impacts on vegetation in the pre- and post-fire events over Iberian Peninsula, Natural Hazards Earth System Sciences, 12, 3123-3137, doi:10.5194/nhess-12-3123-2012, 2012.

Grant O. M., Tronina L., Ramalho J. C., Besson C. K., Lobo-do-Vale R., Pereira J. S., Jones H. G. and Chaves M. M.: The impact of drought on leaf physiology of *Quercus suber* L. trees: comparison of an extreme drought event with chronic rainfall reduction, J. Exp. Bot., 61 (15), 4361–4371, doi: 10.1093/jxb/erq239, 2010.

Griffith, D. A. (Ed.): Spatial Autocorrelation, Elsevier Inc, Texas, 2009.

Grossiord, C., Sevanto, S., Dawson, T. E., Adams, H. D., Collins, A. D., Dickman, L. T., Newman, B. D., Stockton, E. A. and Mcdowell, N. G.: Warming combined with more extreme precipitation regimes modifies the water sources used by trees, New Phytol., doi:10.1111/nph.14192, 2016.

Gu, Y., J. F. Brown, J. P. Verdin and Wardlow, B.: A five-year analysis of MODIS NDVI and NDWI for grassland drought assessment over the central Great Plains of the United States, Geophys. Res. Lett., 34, L06407, doi:10.1029/2006GL029127, 2007.

Guisan, A. and Thuiller, W.: Predicting species distribution: Offering more than simple habitat models, Ecol. Lett., 8(9), 993–1009, doi:10.1111/j.1461-0248.2005.00792.x, 2005.

Hagolle, O., Lobo, A., Maisongrande, P., Duchemin, B. and De Pereira, A.: Quality assessment and improvement of SPOT/VEGETATION level temporally composited products of remotely sensed imagery by combination of VEGETATION 1 and 2 images, Remote Sens. Environ., 94, 172–186, 2005.

Haylock, M. R., Hofstra, N., Klein Tank, A. M. G., Klok, E. J., Jones, P. D. and New, M.: A European daily high-resolution gridded data set of surface temperature and precipitation for 1950-2006, J. Geophys. Res. Atmos., 113(20), doi:10.1029/2008JD010201, 2008.

Hernández-Santana, V., David, T. S. and Martínez-Ferná Ndez, J.: Environmental and plant-based controls of water use in a Mediterranean oak stand, For. Ecol. Manage., 255, 3707–3715, doi:10.1016/j.foreco.2008.03.004, 2008.

Horton, J. L. and Hart, S. C.: Hydraulic lift: a potentially important ecosystem process, Tree, 13(6), 232–235, doi:0169-5347/98, 1998.

Howard, J. and Merrifield, M.: Mapping groundwater dependent ecosystems in California, PLoS One, 5(6), doi:10.1371/journal.pone.0011249, 2010.

Hu, X., Zhang, L., Ye, L., Lin, Y. and Qiu, R.: Locating spatial variation in the association between road network and forest biomass carbon accumulation, Ecol. Indic., 73, 214–223, doi:10.1016/j.ecolind.2016.09.042, 2017.

Huntsinger, L. and Bartolome, J. W.: Ecological dynamics of *Quercus* dominated woodlands in California and southern Spain: A state transition model. Vegetation 99–100, 299–305, 1992.

ICNF: IFN6 – Áreas dos usos do solo e das espécies florestais de Portugal continental. Resultados preliminares., Lisboa, 2013.

Iglesias, A., Garrote, L., Flores, F. and Moneo, M.: Challenges to manage the risk of water scarcity and climate change in the Mediterranean, Water Resour. Manag., 21, 775–788, doi:10.1007/s11269-006-9111-6, 2007.

Joffre, R., Rambal, S. and Ratte, J. P.: The dehesa system of southern Spain and Portugal as a natural ecosystem mimic, Agrofor. Syst., 45, 57–79, doi:10.1023/a:1006259402496, 1999.

Kühn, I.: Incorporating spatial autocorrelation may invert observed patterns, Div and Dist, 13, 66-69, doi:10.1111/j.1472-4642.2006.00293.x, 2007

Kurz-Besson, C., Otieno, D., Lobo Do Vale, R., Siegwolf, R., Schmidt, M., Herd, A., Nogueira, C., David, T. S., David, J. S., Tenhunen, J., Pereira, J. S. and Chaves, M.: Hydraulic lift in cork oak trees in a savannah-type Mediterranean ecosystem and its contribution to the local water balance, Plant Soil, 282(1–2), 361–378, doi:10.1007/s11104-006-0005-4, 2006.

Kurz-Besson, C., Lobo-do-Vale, R., Rodrigues, M. L., Almeida, P., Herd, A., Grant, O. M., David, T. S., Schmidt, M., Otieno, D., Keenan, T. F., Gouveia, C., Mériaux, C., Chaves, M. M. and Pereira, J. S.: Cork oak physiological responses to manipulated water availability in a Mediterranean woodland, Agric. For. Meteorol., 184(December 2013), 230–242, doi:10.1016/j.agrformet.2013.10.004, 2014.

Kurz-Besson, C., Lousada, J. L., Gaspar, M. J., Correia, I. E., David, T. S., Soares, P. M. M., Cardoso, R. M., Russo, A., Varino, F., Mériaux, C., Trigo, R. M. and Gouveia, C. M.: Effects of recent minimum temperature and water deficit increases on *Pinus pinaster* radial growth and wood density in southern Portugal, Front. Plant Sci, 7, doi:10.3389/fpls.2016.01170, 2016.

Li, Y., Jiao, Y. and Browder, J. A.: Modeling spatially-varying ecological relationships using geographically weighted generalized linear model: A simulation study based on longline seabird bycatch, Fish. Res., 181, 14–24, doi:10.1016/j.fishres.2016.03.024, 2016.

Lloret, F., Siscart, D. and Dalmases, C.: Canopy recovery after drought dieback in holm-oak Mediterranean forests of Catalonia (NE Spain), Glob. Chang. Biol., 10(12), 2092–2099, doi:10.1111/j.1365-2486.2004.00870.x, 2004.

López, B., Sabaté, S., Ruiz, I. and Gracia, C.: Effects of Elevated CO2 and Decreased Water Availability on Holm-Oak Seedlings in Controlled Environment Chambers, in Impacts of Global Change on Tree Physiology and Forest Ecosystems: Proceedings of the International Conference on Impacts of Global Change on Tree Physiology and Forest Ecosystems, held 26--29 November 1996, Wageningen, The

Netherlands, edited by G. M. J. Mohren, K. Kramer, and S. Sabaté, pp. 125–133, Springer Netherlands, Dordrecht., 1997.

Lorenzo-Lacruz, J., Garcia, C. and Morán-Tejeda, E.: Groundwater level responses to precipitation variability in Mediterranean insular aquifers, J. Hydrol., 552, 516-531, doi:10.1016/j.jhydrol.2017.07.011, 2017.

Lowry, C. S. and Loheide, S. P.: Groundwater-dependent vegetation: Quantifying the groundwater subsidy, Water Resour. Res., 46(6), doi:10.1029/2009WR008874, 2010.

Lv, J., Wang, X. S., Zhou, Y., Qian, K., Wan, L., Eamus, D. and Tao, Z.: Groundwater-dependent distribution of vegetation in Hailiutu River catchment, a semi-arid region in China, Ecohydrology, 6(1), 142–149, doi:10.1002/eco.1254, 2013.

Maki, M., Ishiahra, M., Tamura, M.: Estimation of leaf water status to monitor the risk of forest fires by using remotely sensed data. Remote Sens. Environ, 90, 441–450, 2004.

Mazziotta, A., Heilmann-Clausen, J., Bruun, H. H., Fritz, Ö., Aude, E. and Tøttrup, A. P.: Restoring hydrology and old-growth structures in a former production forest: Modelling the long-term effects on biodiversity, For. Ecol. Manage., 381, 125–133, doi:10.1016/j.foreco.2016.09.028, 2016.

Mckee, T. B., Doesken, N. J. and Kleist, J.: The relationship of drought frequency and duration to time scales, in AMS 8th Conference on Applied Climatology, pp. 179–184., 1993.

Mendes, M. P., Ribeiro, L., David, T. S. and Costa, A.: How dependent are cork oak (*Quercus suber* L.) woodlands on groundwater? A case study in southwestern Portugal, For. Ecol. Manage., 378, 122–130, doi:10.1016/j.foreco.2016.07.024, 2016.

Middleton, N., Thomas, D. S. G. and Programme., U. N. E.: World atlas of desertification, UNEP, 1992., London., 1992.

Miller, G. R., Chen, X., Rubin, Y., Ma, S. and Baldocchi, D. D.: Groundwater uptake by woody vegetation in a semiarid oak savanna, Water Resour. Res., 46(10), doi:10.1029/2009WR008902, 2010.

Ministério da Agricultura do Mar do Ambiente e do Ordenamento do Território: Estratégia de Adaptação da Agricultura e das Florestas às Alterações Climáticas, Lisbon, 2013.

Montero, G., Ruiz-Peinado, R., Candela, J. A., Canellas, I., Gutierrez, M., Pavon, J., Alonso, A., Rio, M. d., Bachiller, A. and Calama, R.: El pino pinonero (*Pinus pinea* L.) en Andalucia. Ecologia, distribucion y selvicultura, edited by G. Montero, J. A. Candela, and A. Rodriguez, Consejeria de Medio Ambiente, Junta de Andalucia, Sevilla., 2004.

Moran, P. A. P.: Notes on continuous stochastic phenomena, Biometrika, 37(1–2), 17–23 [online] Available from: http://dx.doi.org/10.1093/biomet/37.1-2.17, 1950.

Mourato, S., Moreira, M. and Corte-Real, J.: Water resources impact assessment under climate change scenarios in Mediterranean watersheds, Water Resour. Manag., 29(7), 2377–2391, doi:10.1007/s11269-015-0947-5, 2015.

Münch, Z. and Conrad, J.: Remote sensing and GIS based determination of groundwater dependent ecosystems in the Western Cape, South Africa, Hydrogeol. J., 15(1), 19–28, doi:10.1007/s10040-006-0125-1, 2007.

Nadezhdina, N., Ferreira, M. I., Conceição, N., Pacheco, C. A., Häusler, M. and David, T. S.: Water uptake and hydraulic redistribution under a seasonal climate: Long-term study in a rainfed olive orchard, Ecohydrology, 8(3), 387–397, doi:10.1002/eco.1545, 2015.

Naumburg, E., Mata-Gonzalez, R., Hunter, R., McLendon, T., Martin, D.: Phreatophytic vegetation and groundwater fluctuations: a review of current research and application of ecosystem response modelling with an emphasis on Great Basin vegetation. Environmental Management 35,726-740, 2005.

Neumann, R. B. and Cardon, Z. G.: The magnitude of hydraulic redistribution by plant roots: a review and synthesis of empirical and modeling studies, New Phytol., 194(2), 337–352, doi:10.1111/j.1469-8137.2012.04088.x, 2012.

O'Grady, A. P., Eamus, D., Cook, P. G. and Lamontagne, S.: Groundwater use by riparian vegetation in the wet–dry tropics of northern Australia, Aust. J. Bot., 54, 145–154, doi:10.1071/BT04164, 2006.

Orellana, F., Verma, P., Loheide, S. P. and Daly, E.: Monitoring and modeling water-vegetation interactions in groundwater-dependent ecosystems, Rev. Geophys., 50(3), doi:10.1029/2011RG000383, 2012.

Otieno, D. O., Kurz-Besson, C., Liu, J., Schmidt, M. W. T., Do, R. V. L., David, T. S., Siegwolf, R., Pereira, J. S. and Tenhunen, J. D.: Seasonal variations in soil and plant water status in a *Quercus suber* L. stand: Roots as determinants of tree productivity and survival in the Mediterranean-type ecosystem, Plant Soil, 283(1–2), 119–135, doi:10.1007/s11104-004-7539-0, 2006.

Paço, T.A., David, T.S., Henriques, M.O.; Pereira, J.S., Valente, F., Banza, J., Pereira, F.L., Pinto, C., David, J.S.: Evapotranspiration from a Mediterranean evergreen oak savannah: The role of trees and pasture, J. Hydrol., 369 (1-2), 98–106, doi: 10.1016/j.jhydrol.2009.02.011, 2009.

Paulo, J. A., Palma, J. H. N., Gomes, A. A., Faias, S. P., Tomé, J. and Tomé, M.: Predicting site index from climate and soil variables for cork oak (*Quercus suber* L.) stands in Portugal, New For., 46, 293–307, doi:10.1007/s11056-014-9462-4, 2015.

Peñuelas, J. and Filella, I.: Deuterium labelling of roots provides evidence of deep water access and hydraulic lift by Pinus nigra in a Mediterranean forest of NE Spain, Environ. Exp. Bot., 49(3), 201–208, doi:10.1016/S0098-8472(02)00070-9, 2003.

Pérez Hoyos, I., Krakauer, N., Khanbilvardi, R. and Armstrong, R.: A Review of advances in the identification and characterization of groundwater dependent ecosystems using geospatial technologies, Geosciences, 6(2), 17, doi:10.3390/geosciences6020017, 2016a.

Pérez Hoyos, I., Krakauer, N. and Khanbilvardi, R.: Estimating the probability of vegetation to be groundwater dependent based on the evaluation of tree models, Environments, 3(2), 9, doi:10.3390/environments3020009, 2016b.

Pinto-Correia, T., Ribeiro, N. and Sá-Sousa, P.: Introducing the montado, the cork and holm oak agroforestry system of Southern Portugal, Agrofor. Syst., 82(2), 99–104, doi:10.1007/s10457-011-9388-1, 2011.

Waroux, Y. P. and Lambin, E.F.: Monitoring degradation in arid and semi-arid forests and woodlands: The case of the argan woodlands (Morocco), Applied Geography, 32, 777-786, doi: 10.1016/j.apgeog.2011.08.005, 2012.

QGIS Development Team: QGIS Geographic Information System. Open Source Geospatial Foundation Project., 2017.

R Development Core Team: R: A language and environment for statistical computing. R Foundation for Statistical Computing, Vienna, Austria, 2016.

Rivas-Martínez, S., Rivas-Sáenz, S. and Penas-Merino, A.: Worldwide bioclimatic classification system, Glob. Geobot., 1(1), 1–638, doi:10.5616/gg110001, 2011.

Robinson, T. W.: Phreatophytes, United States Geol. Surv. Water-Supply Pap., (1423), 84, 1958.

Rodrigues, C. M., Moreira, M. and Guimarães, R. C.: Apontamentos para as aulas de hidrologia, 2011

Sabaté, S., Gracia, C. A. and Sánchez, A.: Likely effects of climate change on growth of *Quercus ilex*, *Pinus halepensis*, *Pinus pinaster*, *Pinus sylvestris* and *Fagus sylvatica* forests in the Mediterranean region, For. Ecol. Manage., 162(1), 23–37, doi:10.1016/S0378-1127(02)00048-8, 2002.

Salinas, M. J., Blanca, G. and Romero, A. T.: Riparian vegetation and water chemistry in a basin under semiarid Mediterranean climate, Andarax River, Spain. Environmental Management, 26(5), 539–552, 2000.

Sardans, J. and Peñuelas, J.: Increasing drought decreases phosphorus availability in an evergreen Mediterranean forest, Plant Soil, 267(1–2), 367–377, doi:10.1007/s11104-005-0172-8, 2004.

Sarmento, E. de M. and Dores, V.: The performance of the forestry sector and its relevance for the portuguese economy, Rev. Port. Estud. Reg., 34(3), 35–50, 2013.

Schenk, H. J. and Jackson, R. B.: Rooting depths, lateral root spreads and belowground aboveground allometries of plants in water limited ecosystems, J. Ecol., 480–494, doi:10.1046/j.1365-2745.2002.00682.x, 2002.

Silva, J. S. and Rego, F. C.: Root to shoot relationships in Mediterranean woody plants from Central Portugal, Biologia, 59, 109–115, 2004.

Singer, M. B., Stella, J. C., Dufour, S., Piégay, H., Wilson, R. J. S. and Johnstone, L.: Contrasting water-uptake and growth responses to drought in co-occurring riparian tree species, Ecohydrology, 6(3), 402–412, doi:10.1002/eco.1283, 2012.

Soares, P. M. M., Cardoso, R. M., Ferreira, J. J. and Miranda, P. M. A.: Climate change and the Portuguese precipitation: ENSEMBLES regional climate models results, Clim. Dyn., 45(7–8), 1771–1787, doi:10.1007/s00382-014-2432-x, 2015.

Soares, P. M. M., Cardoso, R. M., Lima, D. C. A. and Miranda, P. M. A.: Future precipitation in Portugal: high-resolution projections using WRF model and EURO-CORDEX multi-model ensembles, Clim Dyn, 49, 2503–2530, doi:10.1007/s00382-016-3455-2, 2017.

Spinoni, J., Vogt, J. V., Naumann, G., Barbosa, P. and Dosio, A.: Will drought events become more frequent and severe in Europe?, Int. J. Climatol., 38(4), 1718–1736, doi:10.1002/joc.5291, 2017.

Stewart Fotheringham, A., Charlton, M. and Brunsdon, C.: The geography of parameter space: an investigation of spatial non-stationarity, Int. J. Geogr. Inf. Syst., 10(5), 605–627, doi:10.1080/02693799608902100, 1996.

Stigter, T. Y., Nunes, J. P., Pisani, B., Fakir, Y., Hugman, R., Li, Y., Tomé, S., Ribeiro, L., Samper, J., Oliveira, R., Monteiro, J. P., Silva, A., Tavares, P. C. F., Shapouri, M., Cancela da Fonseca, L. and El Himer, H.: Comparative assessment of climate change and its impacts on three coastal aquifers in the Mediterranean, Reg. Environ. Chang., 14(S1), 41–56, doi:10.1007/s10113-012-0377-3, 2014.

Stone, E. L. and Kalisz, P. J.: On the maximum extent of tree roots, For. Ecol. Manage., 46(1–2), 59–102, doi:10.1016/0378-1127(91)90245-Q, 1991.

Thornthwaite, C. W.: An approach toward a rational classification of climate, Geogr. Rev., 38(1), 55–94, 1948.

Valentini, R., Scarascia, G. E. and Ehleringer, J. R.: Hydrogen and carbon isotope ratios of selected species of a Mediterranean macchia ecosystem, Funct. Ecol., 6(6), 627–631, 1992.

Vicente-Serrano, S. M., Beguería, S. and López-Moreno, J. I.: A multiscalar drought index sensitive to global warming: The standardized precipitation evapotranspiration index, J. Clim., 23(7), 1696–1718, doi:10.1175/2009JCLI2909.1, 2010.

Vörösmarty, C. J., Green, P., Salisbury, J. and Lammers, R. B.: Global water resources: Vulnerability from climate change and population growth, Science, 289, 284–288, doi:10.1126/science.289.5477.284, 2000.

Xiao R., He X., Zhang Y., Ferreira V. G. and Chang L.: Monitoring groundwater variations from satellite gravimetry and hydrological models: A comparison with in-situ measurements in the mid-atlantic region of the United States, Remote Sensing, 7 (1), 686–703, doi: 10.3390/rs70100686, 2015.

Zomer, R., Trabucco, A., Coe, R., Place, F.: Trees on farm: analysis of global extent and geographical patterns of agroforestry, ICRAF Working Paper-World Agroforestry Centre, 89, doi:10.5716/WP16263, 2009.

Zou, C. B., Barnes, P. W., Archer, S. and Mcmurtry, C. R.: Soil moisture redistribution as a mechanism of facilitation in savanna tree–shrub clusters, Ecophysiology, (145), 32–40, doi:10.1007/s00442-005-0110-8, 2005.

Figure and Table Legends

Table 1: Environmental variables for characterization of the suitability of GDV in the study area.

Table 2: Effect of variable removal in the performance of GWR model linking the Kernel density of *Quercus suber, Quercus ilex* and *Pinus pinea* to predictors Aridity Index (AI); Ombrothermic Index of the summer quarter and the immediately previous month (Ios4); Groundwater Depth (GWDepth); Drainage density (Dd); Slope; and Soil type. The model with all predictors is highlighted in grey and the final model used in this study is in bold.

Table 3: Comparison of Adjusted R-squared and second-order Akaike Information Criterion (AICc) between the simple regression and the GWR models.

Table 4: Classification scores for each predictor. A score of 3 to highly suitable areas and 1 to highly less suitable for GDV.

Table A1: Classification scores for soil type predictor.

Table A2: Correlations between predictor variables and principal component axis. The most important predictors for each axis (when squared correlation is above 0.3) are showed in bold. The cumulative proportion of variance explained by each principal component axis is shown at the bottom of the table.

Figure 01: Study area. On the left the location of Alentejo in the Iberian Peninsula; on the right, the elevation characterization of the study area with the main river courses from Tagus, Sado and Guadiana basins. Names of the main rivers are indicated near to their location in the map.

Figure 02: Large well and piezometer data points used for groundwater depth calculation. Squares represent piezometers data points and triangle represent large well data points.

Figure 03: Map of Kernel Density weighted by cover percentage of *Q. suber, Q. ilex* and *P. pinea*.

Figure 04: Map of environmental layers used in model fitting. (a) – Soil type; (b) – Slope; (c) – Groundwater Depth (Depth); (d) – Ombrothermic Index of the summer quarter and the immediately previous month (Ios4); (e) – Aridity Index (AI).

Figure 05: Spatial distribution of local R^2 from the fitting of the Geographically Weighted Regression.

Figure 06: Spatial distribution of model residuals from the fitting of the Simple Linear model (a) and Geographically Weighted Regression (b).

Figure 07: Map of local model coefficients for each variable. (a) – Aridity Index (AI); (b) - Ombrothermic Index of the summer quarter and the immediately previous month (Ios4); (c) – Groundwater Depth (GWDepth); (d) – Drainage density; (e) - Slope.

Figure 08: Boxplot of GWR model coefficient values for each predictor. AI is Aridity Index; Ios4 is the ombrothemic index of the hottest month of the summer quarter and the immediately previous month; GWDepth is Groundwater Depth and Dd is drainage density.

Figure 09: Suitability map for Groundwater Dependent Vegetation.

Figure 10: Validation map corresponding to the NDWI anomaly considering the months of June, July and August of the extremely dry year of 2005 in the Alentejo area. Brown colors (corresponding to more negative values) indicate vegetation in water stress.

Figure A1: Boxplot of the main predictors used for the Geographically Weighted Regression model fitting (top) and the response variable (below), for the total data (left) and for the 5% subsample (right).

Figure A2: Correlation plot between all environmental variables expected to affect the presence of the Groundwater Dependent Vegetation. Ios1, Ios3 and Ios4 are ombrothermin indices of, respectively, the hottest month of the summer quarter, the summer quarter and the summer quarter and the immediately previous month; Io is the annual ombrothermic index, Spei_extreme and Spei_severe are, respectively, the number of months with extreme and severe Standardized Precipitation Evapotranspiration Index; AI is Aridity index; GWDepth is Groundwater depth, Dd is the Drainage density; Thickness and Soil type refer to soil properties.

Figure B1 – Predictors maps after score classification. (a) – Aridity Index (AI); (b) – Ombrothermic Index of the summer quarter and the immediately previous month (Ios4); (c) – Groundwater Depth (GWDepth); (d) – Drainage density (Dd); (e) – Slope.

Table 1: Environmental variables for the characterization of the suitability of GDV in the study area.

Variable code	Variable type	Source	Resolution and Spatial extent
Slope	**Slope (%)**	This work	0.000256 degrees (25m) raster resolution
Soil type	**Soil type in the first soil layer**	SNIAmb (© Agência Portuguesa do Ambiente, I.P., 2017)	Converted from vectorial to 0.000256 degrees (25m) resolution raster
Thickness	**Soil thickness (cm)**	EPIC WebGIS Portugal (Barata et al., 2015)	Converted from vectorial to 0.000256 degrees (25m) resolution raster
GWDepth	**Depth to groundwater (m)**	This work	0.000256 degrees (25m) raster resolution
Dd	**Drainage Density**	This work	0.000256 degrees (25m) raster resolution
Spei_severe	**Number of months with severe SPEI**	This work	0.000256 degrees (25m) raster resolution Time coverage 1950-2010
SPEI_extreme	**Number of months with extreme SPEI**	This work	0.000256 degrees (25m) raster resolution Time coverage 1950-2010
AI	**Aridity Index**	This work	0.000256 degrees (25m) raster resolution Time coverage 1950-2010
Io	**Annual Ombrothermic Index** Annual average (January to December)	This work	0.000256 degrees (25m) raster resolution Time coverage 1950-2010
Ios1	**Ombrothermic Index of the hottest month of the summer quarter** (J, J and A)	This work	0.000256 degrees (25m) raster resolution Time coverage 1950-2010
Ios3	**Ombrothermic Index of the summer quarter** (J, J and A)	This work	0.000256 degrees (25m) raster resolution Time coverage 1950-2010
Ios4	**Ombrothermic Index of the summer quarter and the immediately previous month** (M, J, J and A)	This work	0.000256 degrees (25m) raster resolution Time coverage 1950-2010

Table 2: Effect of variable removal in the performance of GWR model linking the Kernel density of *Quercus suber, Quercus ilex* and *Pinus pinea* to predictors Aridity Index (AI); Ombrothermic Index of the summer quarter and the immediately previous month (Ios4); Groundwater Depth (GWDepth); Drainage density (Dd); Slope; and Soil type. The model with all predictors is highlighted in grey and the final model used in this study is in bold.

Type	Model	Discarded predictor	AICc	Quasi-global R^2
GWR	Density~ios4 +ai + slope + Dd + GWDepth + soiltype		27389.74	0.926481
GWR	Density~ios4 + slope + Dd + GWDepth + soiltype	Ai	28695.14	0.9085754
GWR	Density~ai + slope + Dd + GWDepth + soiltype	Ios4	28626.88	0.9095033
GWR	Density~ios4 +ai + GWDepth + slope + soiltype	Dd	27909.86	0.9184337
GWR	Density~ios4 +ai + Dd + GWDepth + soiltype	Slope	27429.55	0.924176
GWR	Density~ios4 +ai + Dd + slope+ soiltype	GWDepth	27742.67	0.9208344
GWR	**Density~ios4 +ai + Dd + GWDepth + slope**	**Soiltype 3 levels**	**18050.76**	**0.9916192**

Table 3: Comparison of Adjusted R-squared and second-order Akaike Information Criterion (AICc) between the simple linear regression and the GWR model.

Model	R-squared	AICc	p-value
OLS	0.02	42720	<0.001
GWR	0.99 *	18851	-

*Quasi-global R^2

Table 4: Classification scores for each predictor. A score of 3 was given to highly suitable areas and 1 to highly less suitable areas for GDV.

Predictor	Class	Score
Slope	0%-5%	1
	5%-10%	2
	>10%	3
Groundwater Depth	>15 m	1
	1.5m-15m	3
	≤1.5m	1
Aridity Index	0.6-0.68	1
	0.68-0.75	2
	≥0.75	3
Ios4	<0.28	1
	0.28-0.64	2
	≥0.64	3
Dd	≤0.5	3
	>0.5	1

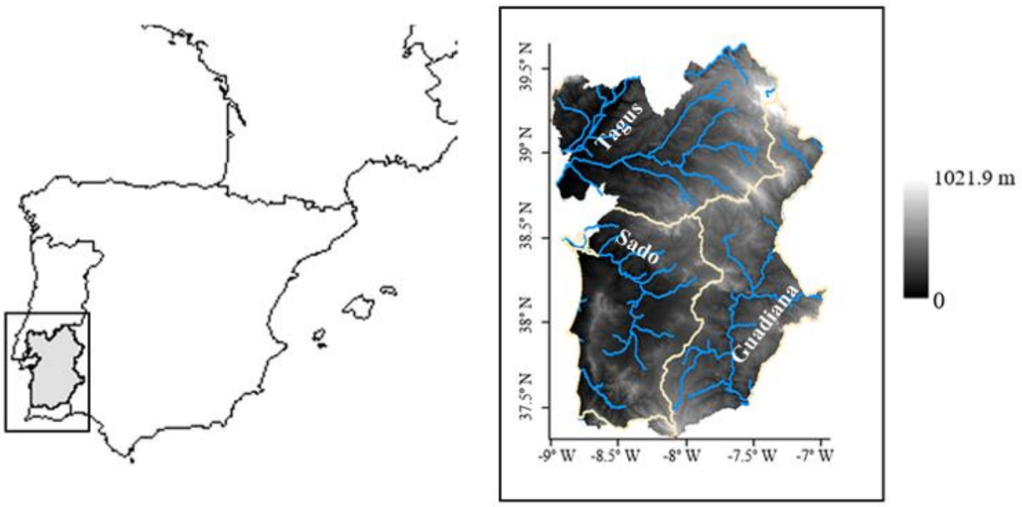

Figure 01: Study area. On the left the location of Alentejo in the Iberian Peninsula; on the right, the elevation characterization of the study area with the main river courses from Tagus, Sado and Guadiana basins. Names of the main rivers are indicated near to their location in the map.

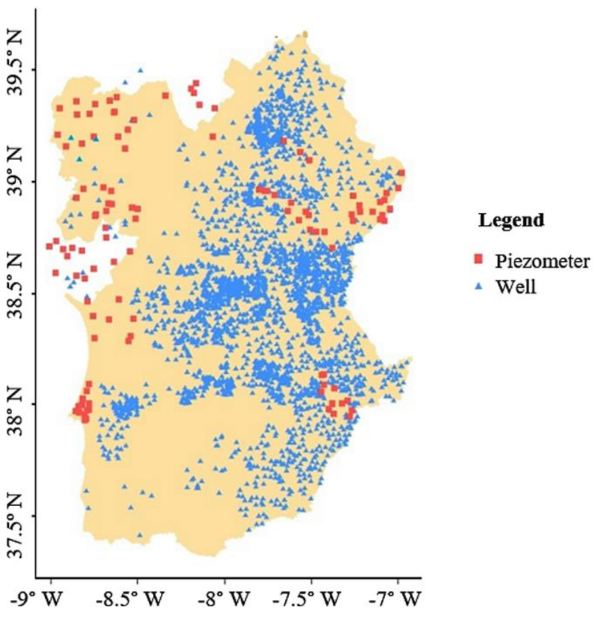

Figure 02: Large well and piezometer data points used for groundwater depth calculation. Squares represent piezometers data points and triangle represent large well data points.

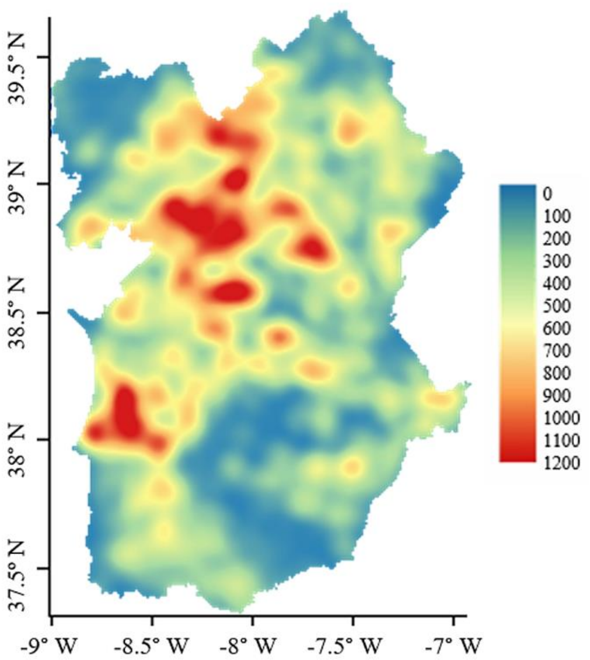

Figure 03: Map of Kernel Density weighted by cover percentage of *Q. suber, Q. ilex* and *P. pinea*.

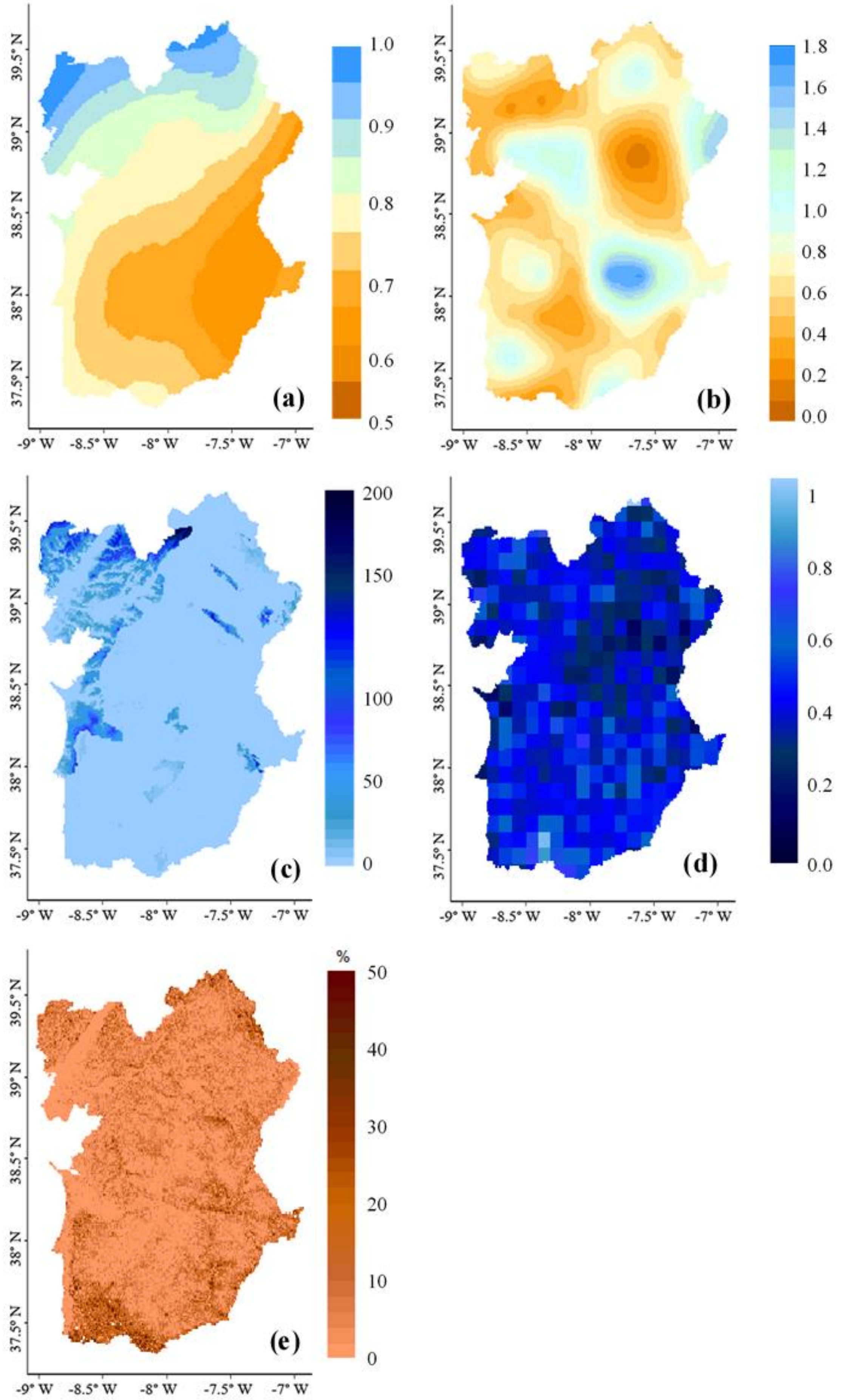
(a)
1.0
0.9
0.8
0.7
0.6
0.5
(b)
1.8
1.6
1.4
1.2
1.0
0.8
0.6
0.4
0.2
0.0
(c)
200
150
100
50
0
(d)
1
0.8
0.6
0.4
0.2
0.0
(e)
%
50
40
30
20
10
0
39.5° N
39° N
38.5° N
38° N
37.5° N
-9° W
-8.5° W
-8° W
-7.5° W
-7° W

Figure 04: Map of environmental layers used in model fitting. (a) – Soil type; (b) – Slope; (c) – Groundwater Depth (Depth); (d) – Ombrothermic Index of the summer quarter and the immediately previous month (Ios4); (e) – Aridity Index (AI).

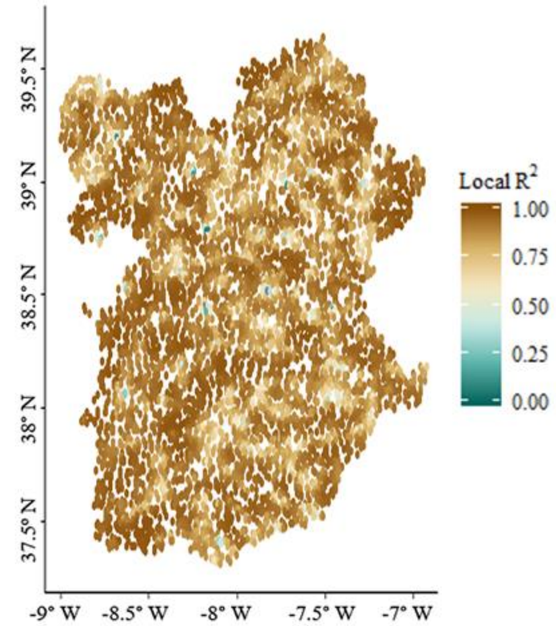

Figure 05: Spatial distribution of local R^2 from the fitting of the Geographically Weighted Regression.

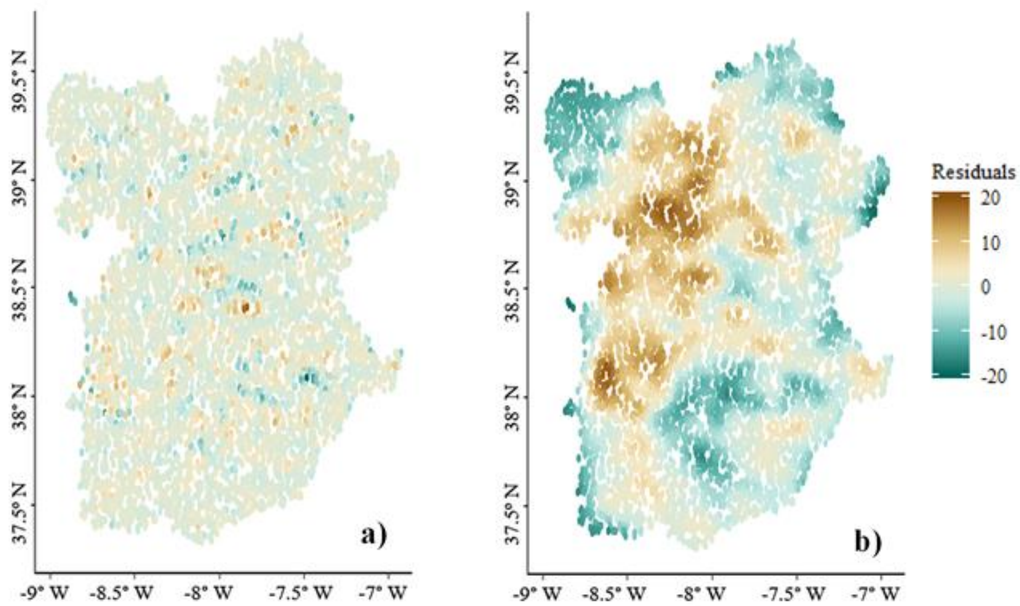

Figure 06: Spatial distribution of model residuals from the fitting of the Geographically Weighted Regression (a) and Simple Linear model(b).

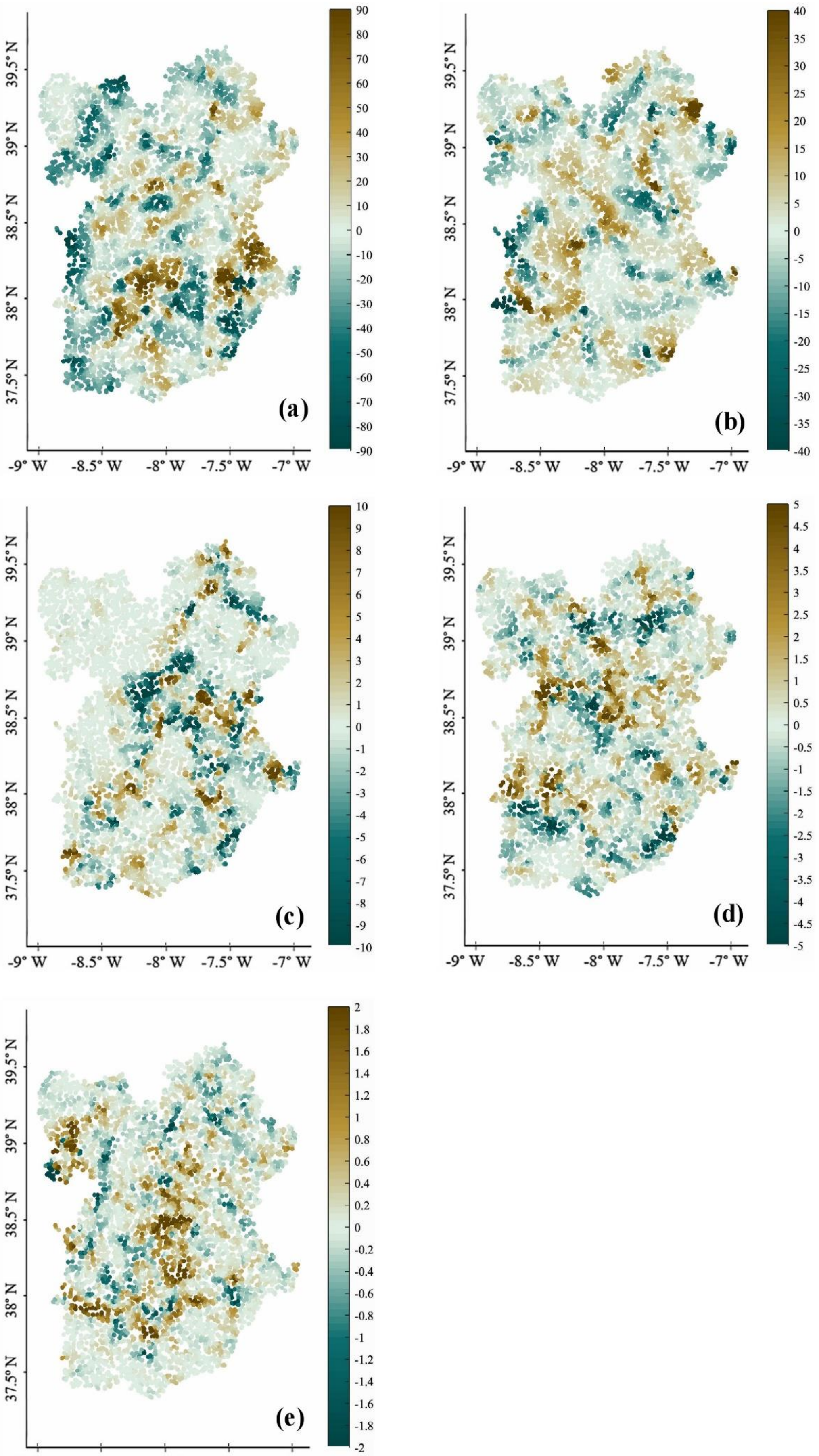

39.5° N
39° N
38.5° N
38° N
37.5° N
-9° W
-8.5° W
-8° W
-7.5° W
-7° W
(a)
90 80 70 60 50 40 30 20 10 0 -10 -20 -30 -40 -50 -60 -70 -80 -90
(b)
40 35 30 25 20 15 10 5 0 -5 -10 -15 -20 -25 -30 -35 -40
(c)
10 9 8 7 6 5 4 3 2 1 0 -1 -2 -3 -4 -5 -6 -7 -8 -9 -10
(d)
5 4.5 4 3.5 3 2.5 2 1.5 1 0.5 0 -0.5 -1 -1.5 -2 -2.5 -3 -3.5 -4 -4.5 -5
(e)
2 1.8 1.6 1.4 1.2 1 0.8 0.6 0.4 0.2 0 -0.2 -0.4 -0.6 -0.8 -1 -1.2 -1.4 -1.6 -1.8 -2

Figure 07: Map of local model coefficients for each variable. (a) – Aridity Index; (b) - Ombrothermic Index of the summer quarter and the immediately previous month (Ios4); (c) – Groundwater Depth (GWDepth); (d) – Drainage density and (e) – Slope.

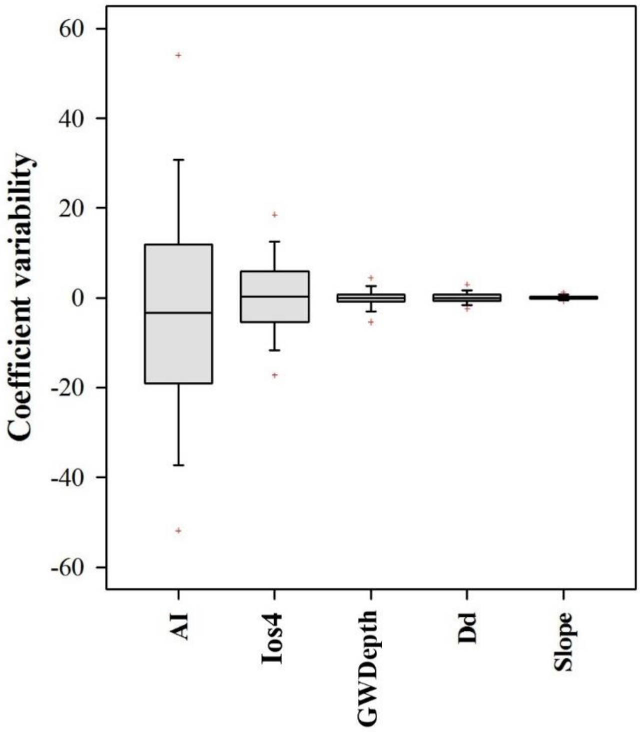

Figure 08 – Boxplot of GWR model coefficient values for each predictor. AI is Aridity Index; Ios4 is the ombrothemic index of the hottest month of the summer quarter and the immediately previous month; GWDepth is Groundwater Depth and Dd is drainage density.

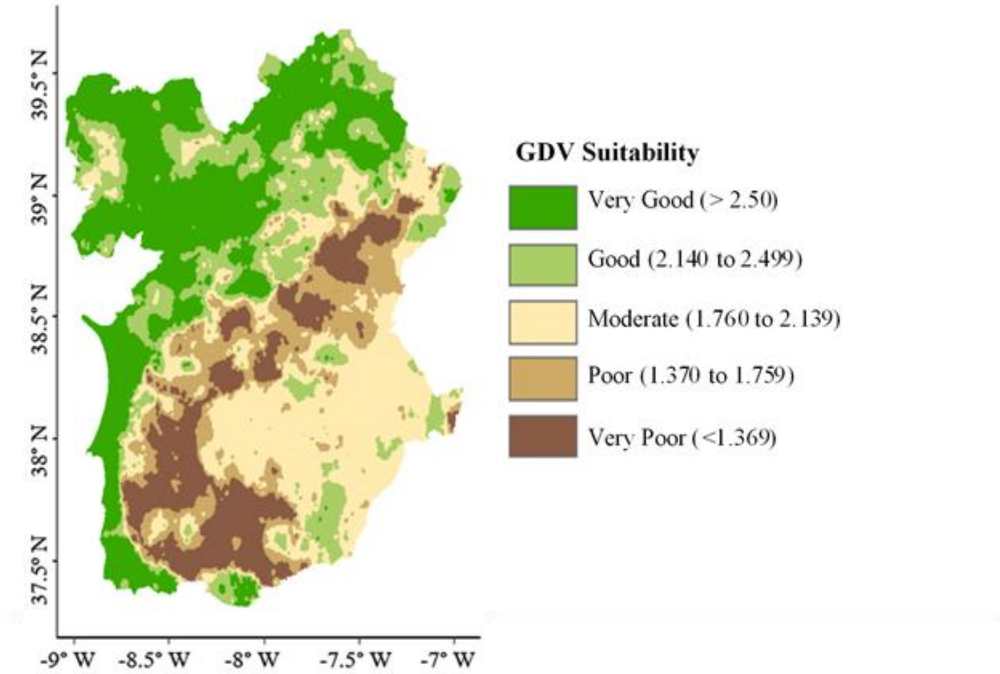

Figure 09: Suitability map for Groundwater Dependent Vegetation.

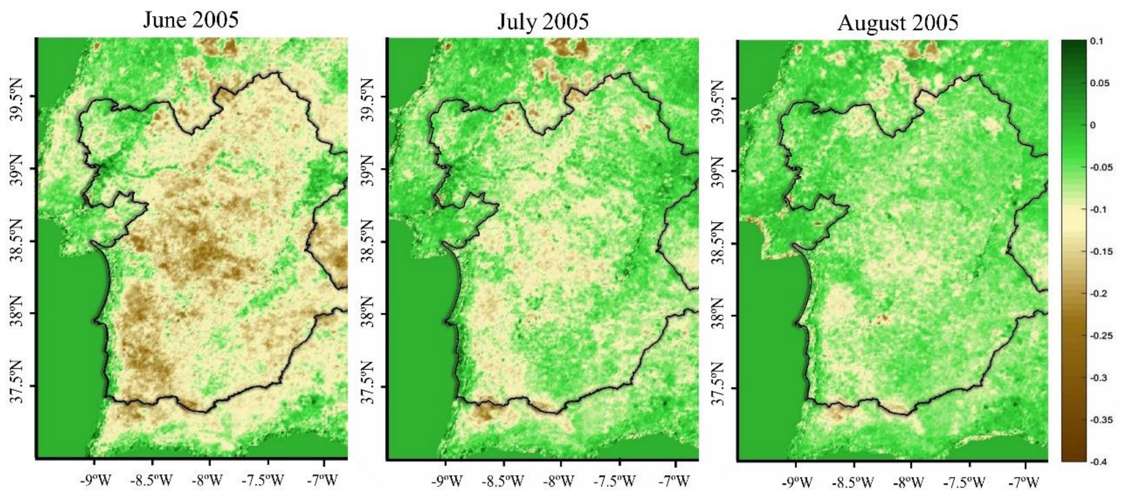

Figure 10: Validation map corresponding to the NDWI anomaly considering the months of June, July and August of the extremely dry year of 2005 in the Alentejo area. Brown colors (corresponding to more negative values) indicate vegetation in water stress.

Appendix A

Table A1: Classification scores for the soil type predictor.

Predictor	Class	Score
Soil type	Eutric Cambisols; Dystric Regosol; Humic Cambisols; Haplic Luvisols; Gleyic Luvisols; Ferric Luvisols; Chromic Luvisols associated with Haplic Luvisols; Ortic Podzols	3
	Calcaric Cambisols; Dystric Regosol associated with Umbric Leptosols; Eutric Regosols; Vertic Luvisols; Eutric Planosols; Cambic Arenosols	2
	Chromic Cambisols; Eutric fluvisols; Chromic Luvisols; Gleyic Solonchak; Eutric Vertisols	1

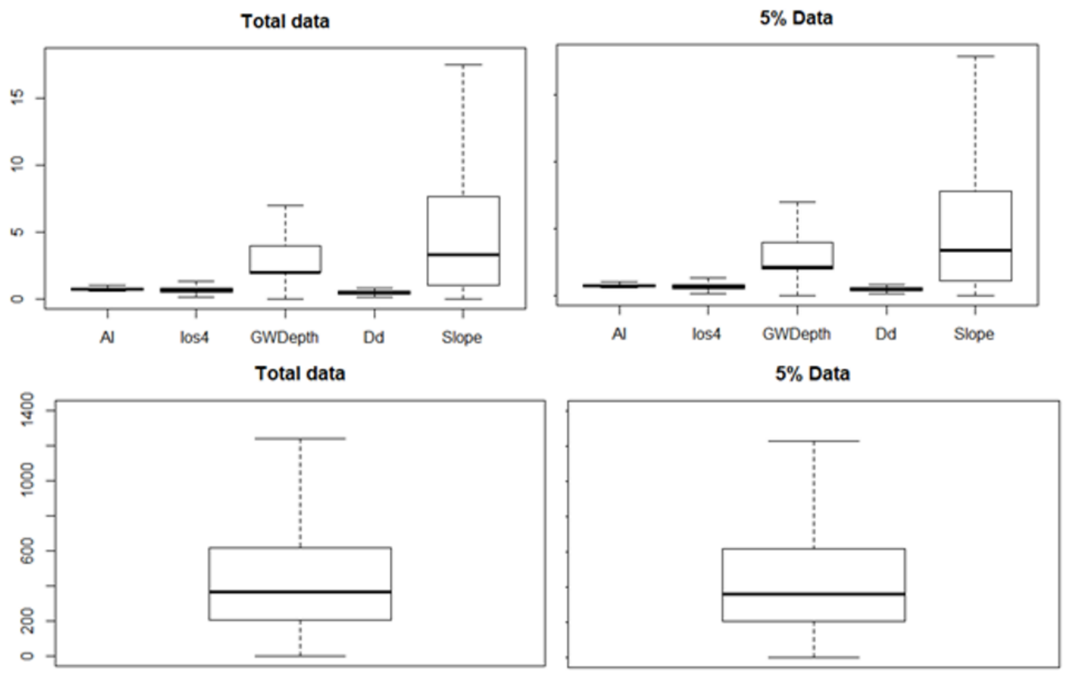

Figure A1: Boxplot of the main predictors for the final Geographically Weighted Regression model fitting (top) and the response variable (below), for the total data (left) and for the 5% subsample (right).

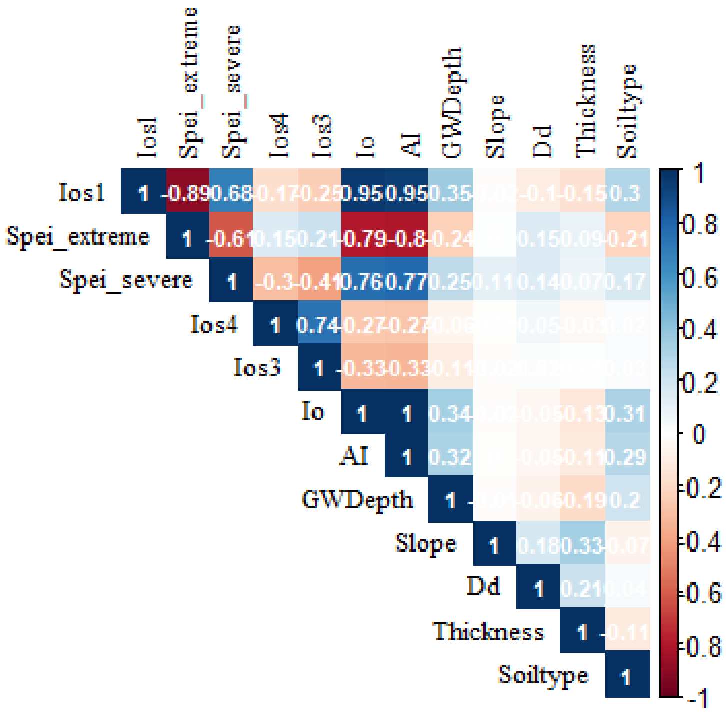

Figure A2: Correlation plot between all environmental variables expected to affect the presence of the Groundwater Dependent Vegetation. Ios1, Ios3, Ios4 are ombrothemic indices of, respectively, the hottest month of the summer quarter, the summer quarter and the summer quarter and the immediately previous month; Io is the annual ombrothermic index, Spei_extreme and Spei_severe are, respectively, the number of months with extreme and severe Standardized Precipitation Evapotranspiration Index; AI is Aridity Index; GWDepth is Groundwater Depth, ; Dd is the Drainage density; Thickness and Soiltype refer to soil properties.

Table A2: Correlations between predictor variables and principal component axis. The most important predictors for each axis (when squared correlation is above 0.3) are showed in bold. The cumulative proportion of variance explained by each principal component axis is shown at the bottom of the table

	PC1	PC2	PC3	PC4	PC5	PC6	PC7	PC8	PC9	PC10	PC11	PC12
Slope	<0.001	**0.32**	0.13	0.06	0.14	0.18	0.18	<0.001	0.03	0.03	<0.01	<0.01
AI	**0.94**	<0.001	0.01	<0.01	<0.001	<0.01	<0.001	<0.001	0.22	**0.33**	**0.40**	**0.68**
Io	**0.93**	<0.01	0.01	<0.01	<0.001	<0.01	<0.001	<0.001	0.24	**0.38**	0.24	**0.72**
Ios1	**0.89**	0.02	0.04	0.01	<0.001	<0.001	<0.001	0.02	0.03	0.14	**0.82**	0.10
Ios3	0.21	0.18	**0.47**	<0.01	<0.01	<0.001	<0.01	0.11	**0.64**	**0.33**	<0.01	<0.01
Ios4	0.15	0.19	**0.53**	<0.001	<0.001	<0.01	<0.001	**0.33**	**0.53**	**0.33**	0.05	<0.01
Spei_severe	**0.66**	0.08	0.01	<0.01	<0.001	-0.02	<0.01	**0.77**	0.08	**0.40**	0.11	0.01
Spei_extreme	**0.72**	0.01	0.04	0.05	<0.01	<0.001	<0.01	**0.36**	**0.44**	0.57	0.29	0.05
GWDepth	0.16	0.05	0.01	**0.33**	0.14	0.26	0.06	0.06	0.04	0.06	0.04	0.01
Dd	<0.01	0.25	0.11	0.20	0.08	**0.32**	<0.01	0.29	0.06	0.04	<0.01	<0.01
Soil type	0.02	0.19	0.03	0.22	**0.46**	0.05	0.02	0.06	0.03	0.05	0.03	<0.01
Thickness	0.02	**0.46**	0.09	0.03	0.06	0.01	**0.32**	0.11	0.03	0.09	0.01	<0.01
Cumulative proportion	0.39	0.54	0.66	0.74	0.81	0.88	0.93	0.96	0.98	0.99	0.99	1

Appendix B

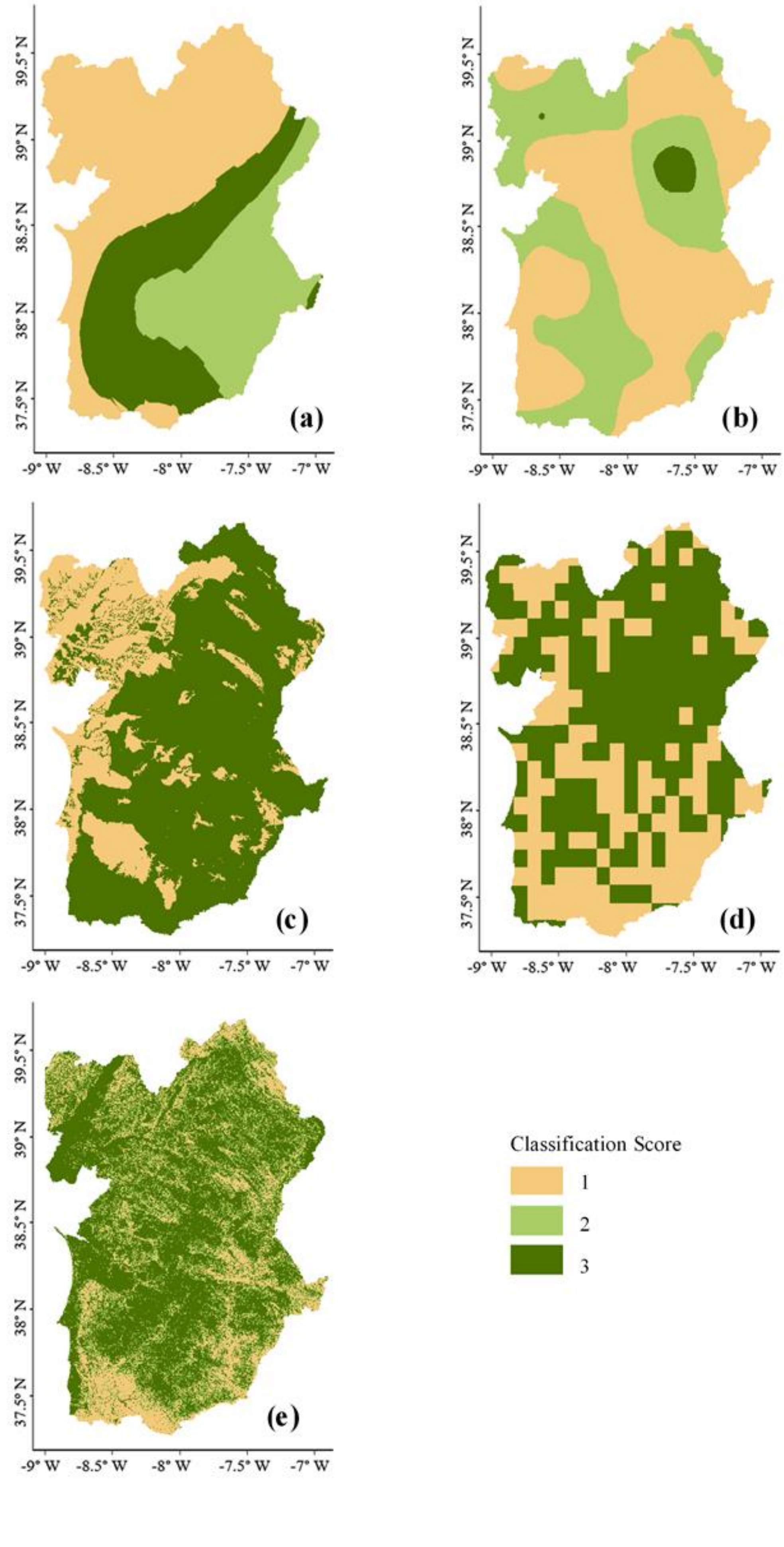

39.5° N
39° N
38.5° N
38° N
37.5° N
-9° W
-8.5° W
-8° W
-7.5° W
-7° W
(a)
(b)
(c)
(d)
(e)
Classification Score
1
2
3

Figure B1 – Predictors maps after score reclassification. (a) – Aridity Index (AI); (b) – Ombrothermic Index of the summer quarter and the immediately previous month (Ios4); (c) – Groundwater Depth (GWDepth); (d) – Drainage density (Dd); (e) – Slope.